

Assessing the applicability of WRF optimal parameters under the different precipitation simulations in the Greater Beijing Area

Zhenhua Di^{1,2} · Qingyun Duan^{1,2} · Chen Wang^{1,2} · Aizhong Ye^{1,2} · Chiyuan Miao^{1,2} · Wei Gong^{1,2}

Received: 7 November 2016 / Accepted: 23 April 2017 / Published online: 13 May 2017
© Springer-Verlag Berlin Heidelberg 2017

Abstract Forecasting skills of the complex weather and climate models have been improved by tuning the sensitive parameters that exert the greatest impact on simulated results based on more effective optimization methods. However, whether the optimal parameter values are still work when the model simulation conditions vary, which is a scientific problem deserving of study. In this study, a highly-effective optimization method, adaptive surrogate model-based optimization (ASMO), was firstly used to tune nine sensitive parameters from four physical parameterization schemes of the Weather Research and Forecasting (WRF) model to obtain better summer precipitation forecasting over the Greater Beijing Area in China. Then, to assess the applicability of the optimal parameter values, simulation results from the WRF model with default and optimal parameter values were compared across precipitation events, boundary conditions, spatial scales, and physical processes in the Greater Beijing Area. The summer precipitation events from 6 years were used to calibrate and evaluate the optimal parameter values of WRF model. Three boundary data and two spatial resolutions were adopted to evaluate the superiority of the calibrated optimal parameters to default parameters under the WRF simulations with different boundary conditions and spatial resolutions, respectively. Physical interpretations of the optimal parameters indicating how to improve precipitation

simulation results were also examined. All the results showed that the optimal parameters obtained by ASMO are superior to the default parameters for WRF simulations for predicting summer precipitation in the Greater Beijing Area because the optimal parameters are not constrained by specific precipitation events, boundary conditions, and spatial resolutions. The optimal values of the nine parameters were determined from 127 parameter samples using the ASMO method, which showed that the ASMO method is very highly-efficient for optimizing WRF model parameters.

Keywords Adaptive surrogate model-based optimization method · Parameter optimization · Optimization assessment · Weather Research and Forecasting model

1 Introduction

Numerical weather prediction (NWP) models have become indispensable tools for studying mesoscale weather processes due to the continuity and predictability of their simulation results (Lorenz 1960; Richardson 2007). In recent decades, NWP models have developed rapidly based on multiple advanced techniques, including supercomputer capability, observational systems, data assimilation, and post-processing, among others. For instance, more observed data obtained by the advanced observation tools have deepened our understanding of certain weather processes, leading to better dynamic representations of physical processes (Cotton et al. 1982; Dudhia 1989; Janjic 1994; Gregory et al. 2000; Chen and Dudhia 2001; Hong and Lim 2006; Gilliam and Pleim 2010). The data assimilation method improves the initial values of the NWP model by merging the observed data with the simulations (Evensen 1997; Barker et al. 2002; Kalnay 2003; Rabier 2005; Wang et al.

✉ Zhenhua Di
zhdi@bnu.edu.cn

¹ State Key Laboratory of Earth Surface Processes and Resource Ecology, Faculty of Geographical Science, Beijing Normal University, Beijing 100875, China

² Institute of Land Surface System and Sustainable Development, Faculty of Geographical Science, Beijing Normal University, Beijing 100875, China

2008; Huang et al. 2009; Liu et al. 2013). Recently, more and more studies started focusing on optimizing parameters of complex NWP models to improve their forecasting skills as the highly-efficient optimization methods arose (Duan et al. 2016; Ollinaho et al. 2014; Yang et al. 2012).

Parameter optimization refers to a process that searches a set of parameter values in the multi-dimensional parameter ranges by the parameter perturbation method, with the intent of bringing the simulation results of a model with the selected parameter values closer to the corresponding observed data (Duan et al. 1994). During parameter optimization, each parameter perturbation produces a new parameter set that is used to update the original model parameter set to carry out new simulations. Therefore, optimization usually requires thousands of model runs using routine optimization methods such as the quasi-Newton method (Liu and Nocedal 1989), the downhill simplex method (Nelder and Mead 1965), simulated annealing (Eglese 1990), and genetic algorithms (Michielssen et al. 1993), among others. However, it is not suitable to tune the parameters of complex NWP model with huge computational demand required. So, earlier studies focused on parameter optimization of relatively simple weather models (e.g., Qiu and Chou 1988; Mu et al. 2002; Severijns and Hazeleger 2005; Duane and Hacker 2008). Even for parameter optimization of complex climate models, simulations at lower spatial resolutions have been conducted to reduce the time consumption of a single model run (Liu et al. 2004; Annan et al. 2005; Bellprat et al. 2012; Ishaish et al. 2012). In recent years, some highly-efficient optimization methods (e.g., Jackson et al. 2008; Wang et al. 2014) were proposed, making it possible to optimize the parameters of complex NWP models. For instance, Yang et al. (2012) optimized the parameters of a cumulus convection parameterization scheme for the Weather Research and Forecasting (WRF) model using multiple very fast simulated annealing (MVFSA) (Jackson et al. 2008). Santanello et al. (2013) used the NASA land information optimization system (LIS-OPT) to adjust the parameters of the Noah land model in the WRF model, which improved the simulation results for the variables related to land-atmosphere interaction. Duan et al. (2016) optimized the sensitive parameters from five physical parameterization schemes of WRF model to improve summer precipitation simulations with 9-km resolutions using adaptive surrogate model-based optimization (ASMO) proposed by Wang et al. (2014).

After the parameter optimization, the problem arises whether the calibrated optimal parameters can still improve the simulation results of model when some simulation conditions are changed. The conditions refer to simulation events, lateral boundary forcing data, and spatial resolutions, among others. If the model with optimal parameters calibrated in last year does not improve the

future forecasting or the optimal parameters calibrated in the high-resolution simulations do not have better simulation ability than the default parameters in the low-resolution simulations, the usefulness of the parameter optimization will be limited. However, note that more attention has been paid to how to obtain the optimal parameters, and the applicability of the optimal parameters across the different simulation conditions is usually ignored. Yan et al. (2014) compared the optimal parameter values of WRF models across three spatial resolutions, but whether the optimal parameters obtained at higher resolutions can improve the simulations at lower resolutions was not discussed. Ollinaho et al. (2014) evaluated the model simulations with optimal parameters under the different geographical distribution and found that the simulated results of surface temperature in Northern Hemisphere get better but worse in Southern Hemisphere and tropics. So, we only analyzed the applicability of the optimal parameters across the different simulation conditions for certain region.

This paper tries to address two problems related to parameter optimization in the NWP model. The first is how to conduct highly efficient parameter optimization of NWP precipitation simulations using the ASMO method. The second is whether the optimal parameters are robust on other simulations of the study area. In this study, the WRF model, as a representative of the complex NWP model, was used to implement parameter optimization for the precipitation simulations. According to the results of the screened sensitive parameters from the parameterization schemes of six physical processes (Di et al. 2016), only the sensitive parameters of the WRF model were optimized by ASMO. The threat score (TS), a common precipitation index used in operational forecasting systems, was used to evaluate the difference between the simulation results and the corresponding observed data. Because a higher resolution WRF simulation was conducted, there was no parameterization scheme to be used to describe the cumulus physical processes. Hence, the optimized parameters are distinctly different from that from experimental design of Duan et al. (2016). After optimization, the applicability of the optimal parameters across precipitation events, boundary conditions, spatial resolutions, and physical processes was examined to demonstrate the robustness of optimal parameters.

This paper is organized as follows. Section 2 presents the methodology related to the ASMO optimization procedure. Section 3 offers a description of the experimental design, including the parameters optimized, the sampling algorithm, the WRF configuration, the selected precipitation events, and the observed data. Section 4 presents the optimization results and discusses the applicability of the optimal parameters under various conditions. Conclusions and further discussion are presented in the last section.

2 Methodology

Compared to routine parameter optimization methods, ASMO method is especially suitable for parameter optimization of large complex dynamic models (e.g., WRF, GCM) with heavy computational requirements. Because the ASMO method searches for the optimal model solution (usually the minimum error between the simulation and the observation), relying mainly on the statistical surrogate model rather than the real physical model, the optimization convergence speed using the ASMO method will be greatly improved. The surrogate model is also called the statistical regression model and is built by a statistical regression method based on the parameter inputs and corresponding output errors of the real physical model. Many regression methods can be selected, such as the multivariate adaptive regression spline (MARS), sum of trees (SOT), support vector machine (SVM), artificial neural networks (ANN), and Gaussian process regression (GPR). The ASMO procedure consists of initial sampling, surrogate model construction, and adaptive sampling. Model parameter optimization of the real physical model using the ASMO method can be simply described as follows.

1. Obtain representative sample sets from the ranges and distributions of the adjusted parameters using a suitable sampling method. Then evaluate the simulation results of the real model with the different parameter sample values and compute their errors by comparing the simulation results with the observed data. The input parameter values and their corresponding model simulation errors are combined to constitute the initial sample points.
2. Build a surrogate model by a statistical regression method among the initial sample points. Note that this usually requires a surrogate model that is more representative of the real model. Hence, the various statistical regression methods should be compared beforehand to determine the best one.
3. Search the optimal parameter values on the surrogate model using the rapid optimization method. Then, as a new parameter set, the optimal parameter values from the surrogate model are substituted into the real physical model to evaluate the corresponding output error of the real model. Finally, new sample point consisting of the new parameter set and its simulated error is added to the initial sample point sets to update the existing surrogate model.
4. Repeat steps (2) and (3) until the convergence criteria for parameter optimization of the real physical model are met. The globally optimal parameter values of the real physical model have now been found.

3 Experimental design

3.1 Model configuration and optimized parameters

The advanced research WRF is a new-generation mesoscale numerical weather prediction model (Skamarock et al. 2008). It serves meteorological applications at scales ranging from tens of meters to thousands of kilometers. WRF version 3.6.1 was used in this study. The simulation domain was located within 38.35°–42.25°N and 113.35°–119.55°E over the Greater Beijing Area in China (i.e., the d02 area in Fig. 1). To obtain a more reasonable lateral boundary data for the d02 area, a two-grid horizontally nested domain was set up. The inner layer is the Greater Beijing Area, which is composed of 180×153 horizontal grid cells with a spatial resolution of 3 km, and the outer layer is the North China area (i.e., the d01 area in Fig. 1), which is composed of 202×145 horizontal grid cells with a spatial resolution of 9 km. The common 38 sigma vertical levels are divided from the surface to 50 hPa. The uniform time step is 60 s. The lateral boundary meteorological fields driving the simulation of the d01 area are 6-hourly interval data from climate forecast system reanalysis (CFSR) data, including surface and radiative fluxes with Gaussian T382 spatial resolution and three-dimensional pressure-level data with a 0.5° grid in latitude and longitude.

To obtain more reasonable precipitation simulations over the Greater Beijing Area, the physical parameterization schemes were chosen to comply with the operational forecasting choices of the Beijing Meteorological Bureau. Hence, the WRF single-moment 6-class (WSM6) microphysics scheme (Hong and Lim 2006), the Kain-Fritsch (new Eta) cumulus scheme (Kain 2004), the rapid radiative-transfer model (RRTM) longwave scheme (Mlawer et al. 1997), the Dudhia shortwave scheme (Dudhia 1989), the Yonsei University (YSU) planetary boundary layer scheme (Hong et al. 2006), the Monin-Obukhov surface layer scheme (Dudhia et al. 1999), and the Noah land-surface model (Chen and Dudhia 2001) were used to constitute the WRF configuration for the physical schemes in this study. Due to the higher spatial resolution (i.e., 3 km) in the d02 area, the cumulus scheme was not used for the inner-layer simulations. However, it had to be considered in the outer-layer simulations with a spatial resolution of 9 km. Finally, based on the WRF parameter sensitivity results of Di et al. (2016), nine parameters from the four physical processes (i.e., the microphysics, shortwave, land-surface, and planetary boundary layer schemes) were selected to tune the precipitation simulation results for the Greater Beijing Area. The nine optimized parameters are listed in Table 1.

Fig. 1 WRF simulation domain with two horizontally nested grids

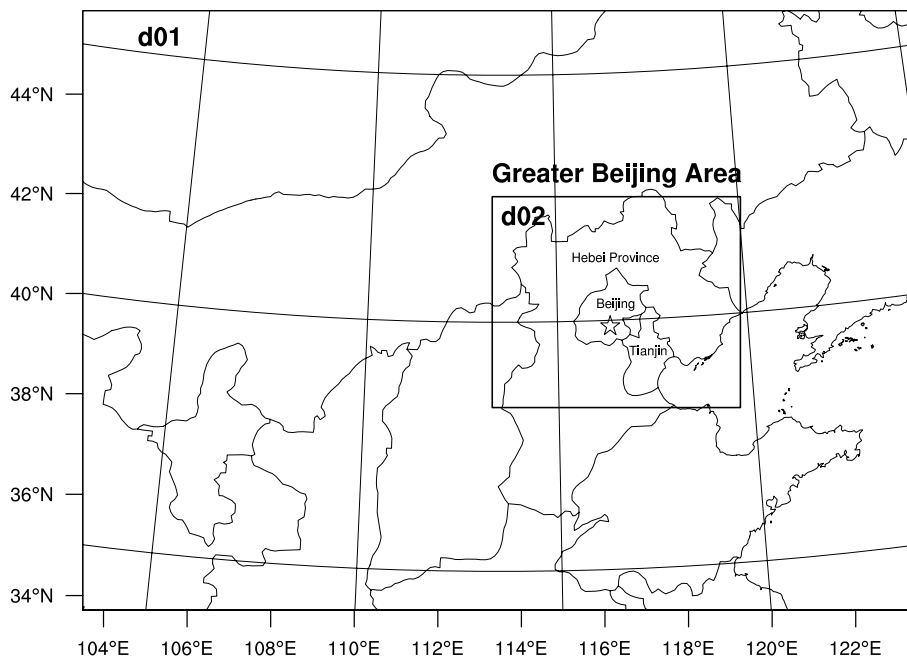


Table 1 The list of the sensitive parameters from four physical schemes of WRF version 3.6.1

Parameter	Scheme	Default	Range	Description
ice_stokes_fac	Microphysics (module_mp_wsm6.F)	14,900	[8000, 30,000]	Scaling factor applied to ice falling velocity (s^{-1})
n0r		$8e^{+6}$	$[5e^{+6}, 1.2e^{+7}]$	Intercept parameter of rain (m^{-4})
dimax		$5e^{-4}$	$[3e^{-4}, 8e^{-4}]$	Limiting maximum value for the cloud-ice diameter (m)
cssca	Short wave radiation (module_ra_sw.F)	$1e^{-5}$	$[5e^{-6}, 2e^{-5}]$	Scattering tuning parameter ($m^2 kg^{-1}$)
porsl	Land surface(module_sf_noahlsf.F)	1	[0.5, 2]	Multiplier for saturated soil water content
bsw		1	[0.5, 2]	Multiplier for Clapp and Hornberger “b” parameter
brcr_sb	Planetary boundary layer (module_bl_ysu.F)	0.25	[0.125, 0.5]	Critical Richardson number for the boundary layer of land
pfac		2	[1, 3]	Profile shape exponent used to calculate the momentum diffusivity coefficient
sm		15.9	[12, 20]	Counter-gradient proportional coefficient of non-local momentum flux

3.2 Observed data and precipitation events

Summer precipitation events from 2008 to 2010 in the Greater Beijing Area were selected to conduct WRF parameter optimization. The observed data came from China hourly merged precipitation analysis products (CHMPA-Hourly, version 1.0), which combines 30,000 gauge stations and the climate precipitation center morphing (CMOPRH) satellite precipitation product at a horizontal resolution of 0.1° in latitude and longitude (Shen et al. 2014).

Based on observed data, the daily average precipitation amounts for the Greater Beijing Area over summer (JJA) from 2008 to 2010 are shown in Fig. 2. From these, nine precipitation events, including the maximum precipitation event for each month, were selected to conduct the optimization experiments for obtaining the better WRF parameter

value for precipitation simulations; except that, another six precipitation events, including the second strongest precipitation events, were selected to conduct the validation of the optimal parameter values. Each of all 15 events spanned 2 days. Therefore, the nine optimization events were framed by boxes (a–i) with solid borders, and the other six validation events were framed by boxes (A–F) with dotted borders in Fig. 2. Besides the 15 precipitation events, 20 summer (JJA) precipitation events from 2011 to 2013 were also simulated to validate the reasonableness of the optimal parameters.

3.3 Experimental setup for parameter optimization

The ASMO method was used to optimize the nine sensitive parameters. The method is available in a software package

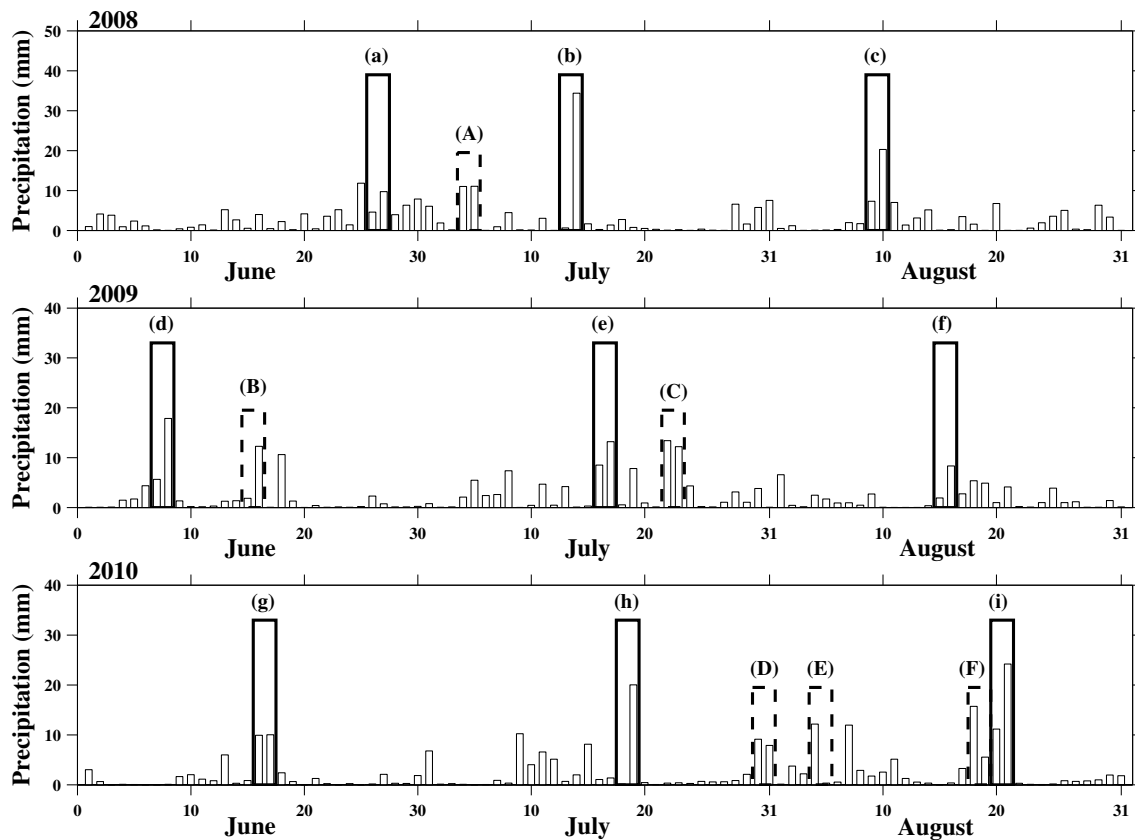


Fig. 2 The 15 precipitation events, including the maximum precipitation in each month during the summer from 2008 to 2010. The events were divided into two categories: (1) the calibration events,

framed by boxes (a–i) with solid border; (2) the validation events, framed by boxes (A–F) with dotted border

called the uncertainty quantification Python laboratory (UQ_PyL) (Wang et al. 2016). UQ_PyL integrates many tools for uncertainty quantification (UQ), including design of experiments, statistical analysis, sensitivity analysis, surrogate modeling, and optimization. Parameter optimization for the WRF model using ASMO required four steps. First, the adjusted parameters were sampled according to their ranges and distributions to obtain the initial parameter sets. If the parameter distributions are unknown, it is usually assumed that the parameter follows a uniform probability distribution according to the maximum entropy or minimum relative entropy theory (Woodbury and Ulrych 1993; Hou and Rubin 2005). Under the assumption, it has been proved that a quasi-Monte Carlo (QMC) sampling method can achieve better uniformity in higher-dimensional projections (Hou et al. 2012; Wang et al. 2014). Jones et al. (1998) suggested that the sample size for the initial parameter sets should be 10 times the dimensionality of the parameters. Hence, 100 points in nine-dimensional parameter space, as selected using the QMC sampling method in this study, were sufficient. Second, all the simulation errors of the WRF models with the 100 different parameter sets were evaluated, and then a statistical surrogate model was constructed using a reasonable statistical regression

method based on 100 combinations of parameter inputs and corresponding model output errors. Wang et al. (2014) and Gong et al. (2015) found that the Gaussian process regression (GPR) method had better regression ability than the other methods (e.g., SVM, MARS, ANN, and random forests, among others), and therefore the GPR method was chosen to construct the surrogate model. Third, to optimize the surrogate model, the more efficient shuffled complex evolution (SCE-UA) optimization method (Duan et al. 1994) was used to search for the optimal parameter values of the surrogate model. As a new parameter set, the optimal parameter values were put into the real WRF model to obtain the corresponding simulation error. The new parameter set and its simulation error were added to the initial sample sets to update the existing surrogate model. Finally, the two processes (optimization and update of the surrogate model) were repeated until the convergence criteria for WRF model parameter optimization were met. In this study, the convergence criteria were defined as either the local optimal value of WRF simulation remaining unchanged after a number of searches equal to five times the dimensionality of the parameters, or the number of searches reaching the prescribed maximum number of samples.

The evaluation function for the precipitation simulation results was the threat score (TS), which can be formulated as follows:

$$TS = \frac{NA}{NA + NB + NC}, \tag{1}$$

where NA is the number of grid cells where the simulated and observed precipitation amounts simultaneously fall into the prescribed threshold range; NB is the number of grid cells where the simulated value falls within the range, but the observed value does not; and NC is the number of grid cells where the simulated value does not fall within the range, but the observed value does. The range of TS is from 0 to 1, where 0 indicates no score, and 1 indicates a perfect score. To evaluate the precipitation simulation results more precisely, the 6-hourly TS were used rather than the 24-hourly TS. According to the classification of 6-hourly precipitation intensity in Table 2, the TS formulation in Eq. (1) was used to compute the hit rates for the various threshold intervals. Because of the lower occurrence rates for heavy storm and severe storm among the selected precipitation events according to the observation date, simulations for the first four types of precipitation (i.e., light rain, moderate rain, heavy rain, and storm) were considered in this study.

To obtain better forecasts of the four types of precipitation, multi-objective optimization was used. According to the strategy proposed by Liu et al. (2005) to solve multiple-objective optimization problems, the multi-objective cost functions were converted to a single-objective cost function by a weighted sum method that allocated the different weights to multiple single-objective functions and then summed them. In this study, the total weighted objective function for the four precipitation types was defined as follows:

$$F(\theta) = -\frac{1}{4} \sum_{j=1}^4 \frac{f_j(\theta)}{f_j(\theta_{def})}, \tag{2}$$

where $f_j(\theta)$ is the TS value of the simulation with input parameter values θ for the j th type of precipitation; j is equal to 1, 2, 3, or 4, representing light rain, moderate rain,

heavy rain, and storm, respectively; θ_{def} is a constant representing the default parameter values; and the ratio of $f_j(\theta)$ to $f_j(\theta_{def})$ is the normalized TS for parameter values θ for the j th type of precipitation. Taking the 100 initial sample points as an example, the average values of all normalized TS for light rain, moderate rain, heavy rain, and storm were 1.013, 1.031, 1.089, and 0.964, respectively. Therefore, equal weights (i.e., $\frac{1}{4}$) were divided into the respective normalized TS in the total multi-objective function. Higher TS value indicates better precipitation forecasting according to the definition of TS, and hence the negative sign means that better simulations have smaller values of total normalized TS.

Besides TS, another quantitative assessment index for the validation of precipitation optimization simulations is the structure, amplitude, and location (SAL) index proposed by Wernli et al. (2008). They describe the difference between simulated and observed precipitation fields under the different aspects. Structure (S) represents the difference between simulation results and observations using the ratio of total to maximum precipitation. It captures information on the size and shape of the precipitation field. Negative values of S usually occur in cases with fewer forecasts for the precipitation area or more forecasts of the maximum precipitation amount. Amplitude (A) corresponds to the simulation bias because it represents the normalized difference between the average precipitation amounts in the simulated and observed precipitation fields. A negative value for A means that the simulated amounts are less than the observed amounts. Location (L) refers to the normalized distance between the centers of gravity of the simulated and observed precipitation fields. It includes two parts, the first being the normalized distance between the centers of gravity of the total simulated and observed precipitation fields, and the second being the difference of the normalized weighted averaged distances, which is computed by taking the distances between the centers of gravity of the total and each individual precipitation field, each of these for both simulated and observed precipitation fields. The closer the values of S , A , and L are to zero, the better are the simulated results.

Table 2 Precipitation intensity classification criteria

Precipitation ranks	6-hourly precipitation amount range (mm)
Light rain	[0.1, 4.0)
Moderate rain	[4.0, 13.0)
Heavy rain	[13.0, 25.0)
Storm	[25.0, 60.0)
Heavy storm	[60.0, 150.0)
Severe storm	[150.0, 350.0)

4 Results and analysis

4.1 Optimization results and analysis

4.1.1 The optimization effect and speed of WRF precipitation simulation using ASMO

After optimizing the nine WRF model parameters using ASMO, the objective function value from formulation (2) was reduced from -1.0 with the default parameter values

to -1.141 with the optimal parameter values. The minimum value for the 100 initial samples was -1.092 , which was less than the objective function value with the default parameters. The adaptive optimization speed of the WRF model for the total normalized TS using ASMO is shown in Fig. 3. It can be seen that about 27 new parameter samples were generated based on the 100 initial samples to meet the optimization convergence criterion. The last minimum value appeared at the 127th sample point. After that, 45 new samples did not further reduce the total objective function value, and therefore the optimization convergence criterion was met according to the previous definition.

4.1.2 Comparison of TS values for WRF precipitation simulations by the optimization

After parameter optimization of the WRF model for simulation of summer precipitation in the Greater Beijing Area using ASMO, the optimal parameter values of the WRF model over the region were finally obtained. Next, comparisons of TS values for WRF precipitation simulations with the optimal parameters against the default parameters were conducted to validate the optimization effect. The TS results of WRF simulations with both default and optimal parameters for calibrated events (a–i) are shown in Fig. 4. It is apparent that the average percentage improvements of TS values for light rain, moderate rain, heavy rain, and storm were 6.97, 22.26, 28.07, and 1.02%, respectively. These results show that the optimal WRF parameters obtained by AMSO can greatly improve summer precipitation simulations in the Greater Beijing Area. However, the simulations for storm showed little improvement. This problem was caused by the definition of the multi-objective functions in formulation (2), where the normalized TS for the four types of precipitation were assigned equal weights. This

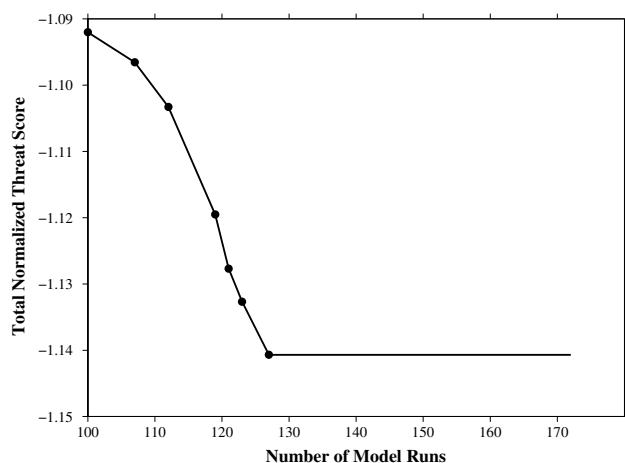


Fig. 3 Convergence speed of the parameter optimization for the WRF model using the ASMO method

scheme was meant to ensure that the simulation results of all four types of precipitation would be better, and therefore it is acceptable that the simulation results for three types of precipitation were significantly improved, whereas those for storm showed little improvement. If much more weight had been assigned to the single objective function for storm in formulation (2), the simulation results for storm would have shown distinct improvement.

Figure 5 show a comparison of TS values of the optimization simulations with the two different weighted objective functions for Event (c) in calibration events. “Opt1” represents the optimization of Event (c) using the equal weighted objective function [i.e., Formulation (2)]. The second optimization for Event (c) used the unequal weighted objective function and was defined as “Opt2”. The weights of light rain, moderate rain, heavy rain, and storm in the unequal weighted objective function were assigned as 0.1, 0.1, 0.1, and 0.7, respectively. We found that the percentage improvements for storm by optimization varied from -2.75 – 11.05% when its weight in objective function was assigned from 0.25 to 0.7, which indicates that the optimization for storm will be significantly improved if the much more weights are assigned to the storm in the multi-objective optimization function. By the comparison of “Opt1” and “Opt2”, we also found that the improvements for other types of precipitation simulations would be reduced if much more weights were assigned to the storm.

In fact, many studies have pointed out that a true multiple-objective optimization method should construct a Pareto surface made up of all the optimal values of the various weighted objective functions (Gong et al. 2016). In Fig. 4, the simulations for all four types of precipitation were improved, which indicates that the setup of the overall objective function is reasonable and can provide positive feedback to the four single objective functions (i.e., the normalized TS). Not only were total precipitation simulation results for all nine events improved, but also most of the simulation results for single precipitation events were also improved for the four precipitation types. Negative optimization percentages tended to be associated with events with lower TS values or less than 10% losses. Moreover, after 127 re-samplings, better simulation results were obtained than with the default parameters. Therefore, it can be concluded that the ASMO method is a highly-efficient way to optimize WRF model parameters.

4.1.3 Comparison of precipitation spatial distributions by the optimization

In addition to a comparison of total precipitation amounts with the TS index, the simulation results for spatial

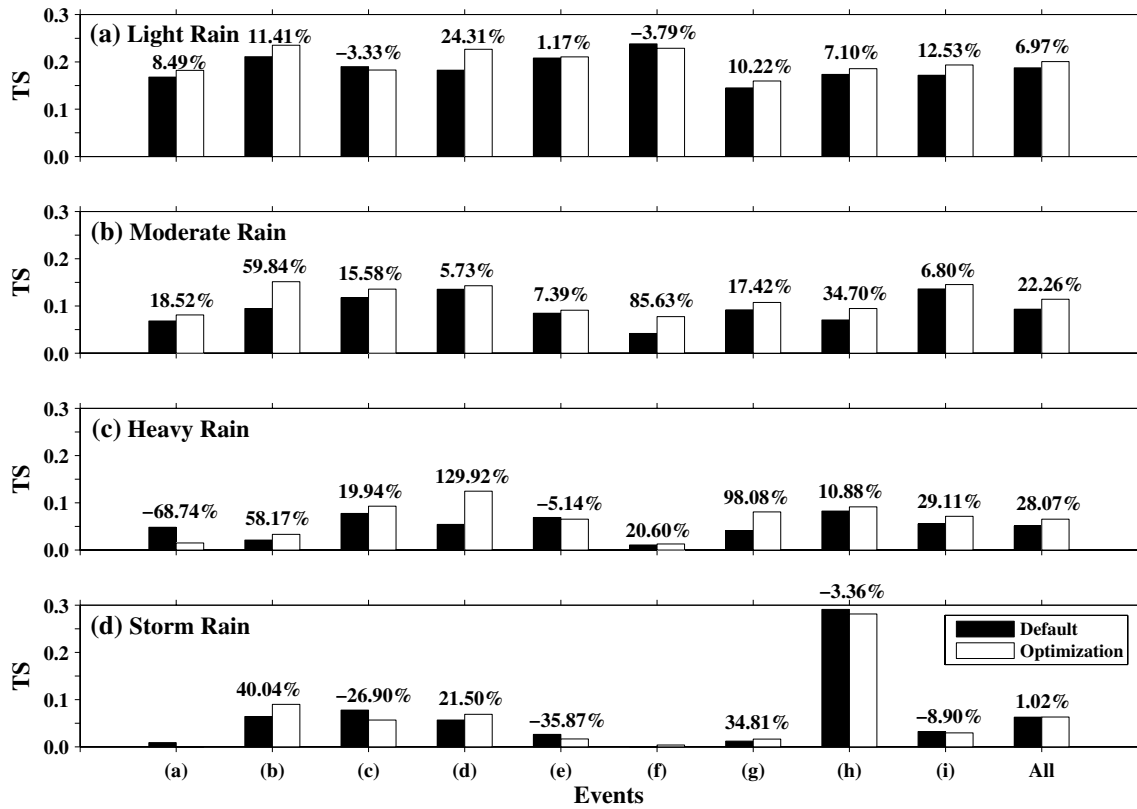


Fig. 4 Comparison of TS values of four types of precipitation simulations using optimal and default parameters for calibration events from 2008 to 2010. The *x-axis* represents precipitation events for the

calibration period in the Greater Beijing Area, and the *y-axis* represents the TS values of the simulated data compared with observed data

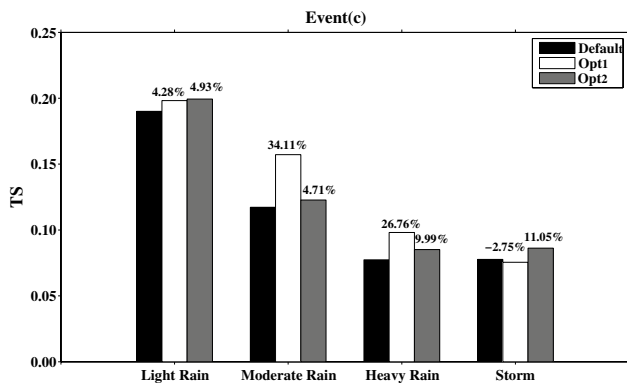


Fig. 5 Comparison of TS values of the optimization simulations with the two different weighted objective functions for Event (c). *Opt 1* and *Opt 2* used the equal and unequal weighted objective functions, respectively

To match them with observed data, the WRF simulation results with 3-km spatial resolution were interpolated to the grid cells with a spatial resolution of 0.1°. For the default and optimal parameters, the bias between the simulation results and the observed data is shown in Fig. 6b, c, respectively. Figure 6 shows two significant improvements in strong precipitation areas. One is the strongest precipitation area, marked by the deep red color in Fig. 6a and occurring in the southeast region along the coastline of China. For the strongest precipitation area, the simulation biases with the optimal parameter values were significantly smaller. The other area is the second strongest precipitation area, marked by the orange color in Fig. 6a, across the southern border between Beijing City and Hebei Province. There was also a distinct improvement in simulated precipitation amounts for the second strongest precipitation area. This means that the simulations with optimal parameter values can provide more accurate precipitation forecasting than the original simulations with default parameter values, especially for high-precipitation areas. This demonstrates the usefulness of improving WRF model simulation results using optimal parameter values. Note also that no obvious improvement was seen in the Bohai Sea, located in the southeastern

distributions of daily average precipitation for the nine calibrated events are shown in Fig. 6. Figure 6a gives the spatial distribution of observed precipitation obtained by averaging precipitation data for all nine events (i.e., 18 days) in each grid cell of 0.1° × 0.1° latitude and longitude.

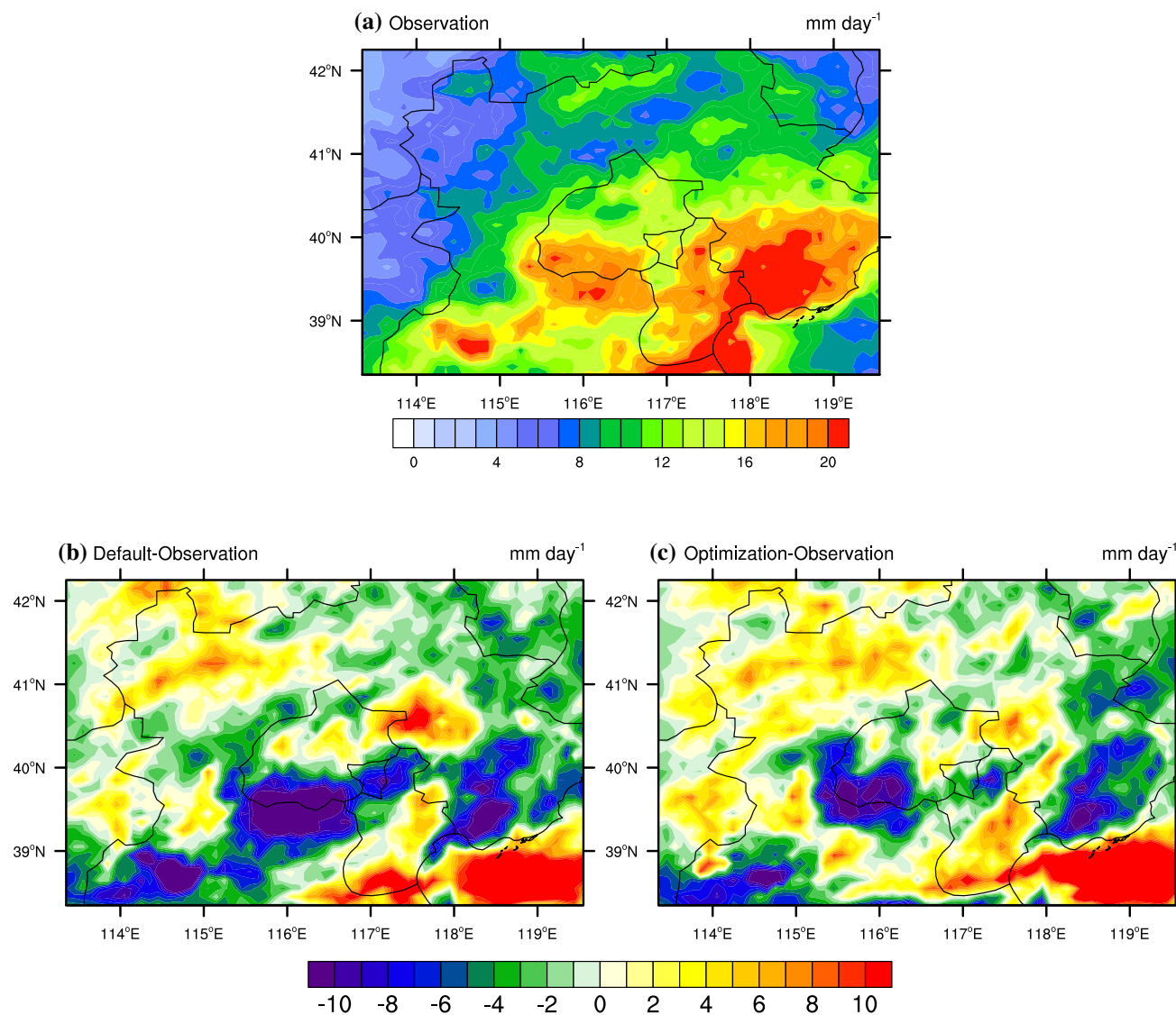


Fig. 6 Spatial distributions of precipitation for all the calibration events: **a** observed precipitation amounts; **b** difference between WRF simulations with default parameters and observed values; **c** difference between WRF simulations with optimal parameters and observed values

corner of the study area; this was related to the lack of precipitation observation stations and inaccuracy of sea temperature forcing data in the Bohai Sea.

Besides the total spatial distributions of daily average precipitation for nine calibrated events, the spatial distributions of daily average precipitation for nine single calibrated cases were also compared to analyze how the optimized parameters improve the simulation of single case. There are two representative cases to be given and their comparisons of the simulations with default and optimal parameters are shown in Fig. 7. Event (h) has an obvious improvement and Event (b) has little improvement in all nine precipitation events. Compared with the default simulation results, the optimal parameter values have a significant improvement on the simulation of storm (marked red in Fig. 7b) for Event (h). The

precipitation pattern of the optimization results is closer to the observation compared with the default simulation results. The conclusions are consistent to those of the comparisons for the total precipitation simulations. Event (b) is one of the little improved cases, because the optimal parameter values extended the storm band simulated by the default simulation northward a little, but the observed precipitation bands in the north and south of Hebei Province were not still captured by the optimization simulation.

4.1.4 Comparison of SAL between the default and optimization precipitation simulations

An SAL comparison of the total simulated precipitation fields with default and optimal parameters for the nine

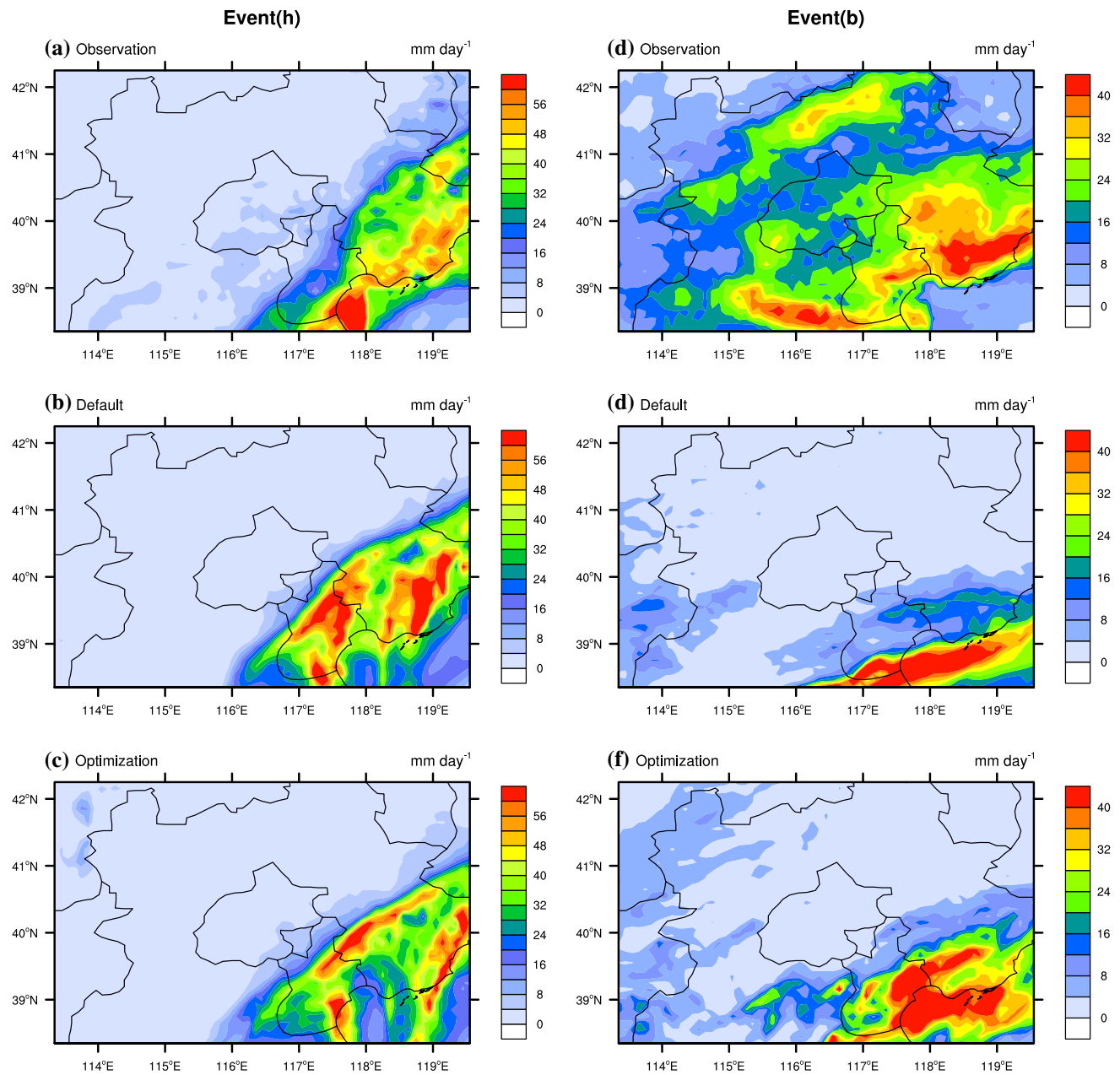


Fig. 7 Spatial distributions of precipitation for two events (**h**) and (**b**) of the nine calibration events. Event (**h**) has an obvious improvement and Event (**b**) has little improvement in all nine calibration events

events (a–i) is shown in Fig. 8. Overall, it was found that the SAL values of the simulation results with the optimal parameter values were closer to zero than those of the simulation results with the default parameter values, which demonstrates that using the optimal WRF model parameters is a valid way to improve simulation results for summer precipitation in the Greater Beijing Area. By combining these results with those shown in Fig. 6, it was concluded that the negative values of S occurred in Fig. 8 mainly because the simulated equivalent precipitation amounts

with default parameters were lower than the observed values. With parameter optimization, the simulated maximum precipitation amount occurred in the south of Tianjin City has been reduced from 40.48 to 29.96 mm day^{-1} which is closer to the observed value. Meanwhile, the total precipitation amounts increased, as shown in Fig. 6. These results bring the increase of S according to the definition of the structure index S . With parameter optimization, A varied from negative to positive values, which indicates that the average precipitation amounts in the optimized simulation

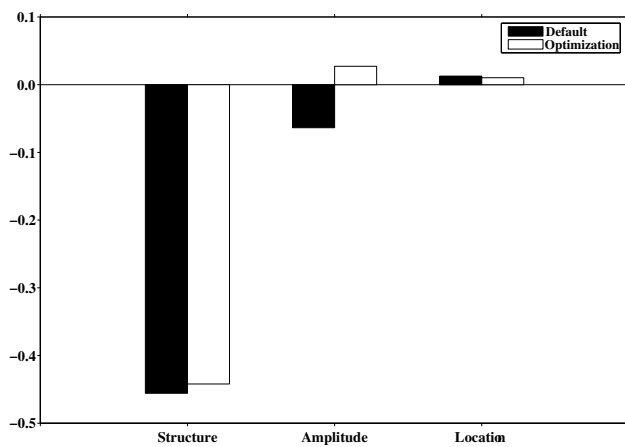


Fig. 8 Comparison of structure (S), amplitude (A), and location (L) of precipitation simulations of the calibration events using default and optimal parameters

were greater than the observed data based on the definition of A . The A value for the optimized simulation was 0.027, which is obviously smaller than the absolute value of A (-0.06) for the default simulation. The L value for the optimized simulation was smaller than that for the default simulation, which indicates that the location of the rain band was moved closer to the observed rain band. The SAL comparison further verifies the reasonableness of the parameter optimization for the WRF model.

4.2 Impact of the optimal parameters on simulations of other precipitation events

4.2.1 Validation of summer precipitation event simulations from 2008 to 2010

One of the important issues for verifying the applicability of the optimal parameter values is whether the optimal WRF model parameter values obtained by the parameter calibration for the precipitation events (a–i) will still work for the simulations of the new validation events (A–F) shown in Fig. 2. Therefore, the WRF model with the optimized parameter values was used to simulate the precipitation amounts of the validation events (A–F). Then the results were compared with the corresponding simulation results from the WRF model with the default parameters. Figure 9 shows a comparison of the TS values of the four types of precipitation simulations for events (A–F) using the optimal and default parameter values. The TS values of the optimized simulations also showed significant improvement over those of the default simulations. The percentage improvements for light rain, moderate rain, heavy rain, and storm were 8.14, 5.84, 19.09, and 7.26%, respectively. Moreover, only the TS value of the storm in the (C) event

significantly decreased in the optimized WRF simulations. However, this does not change the conclusion that the WRF model with optimal parameters obtained by ASMO improved the precipitation forecasting of other events from 2008 to 2010 in the Greater Beijing Area.

The SAL measure was also used to evaluate the precipitation simulation results for validation events (A–F). Figure 10 shows a comparison of the SAL values for WRF simulations of the validation events (A–F) with the optimal and default parameter values. It is evident that the absolute values of S , A , and L for the WRF simulations with optimal parameter values are smaller than those of the WRF simulations with default parameter values, which indicates that the WRF simulation results with optimal parameter values are closer to observations for precipitation events (A–F) during the validation period, according to the definitions of S , A , and L . Overall, it has been demonstrated that the WRF model with the optimal parameter values obtained by ASMO can obtain better summer precipitation forecasting than WRF model with the default parameters over the Greater Beijing Area from 2008 to 2010. However, are the optimized WRF model parameter values superior to the default parameter values for predicting summer precipitation for other years in the Greater Beijing Area? This question will be addressed in the next section.

4.2.2 Validation of summer precipitation event simulations from 2011 to 2013

To validate further the applicability of the optimal parameters on different precipitation events, the precipitation events from 2011 to 2013 were simulated to compare the results of WRF models using optimal and default parameter values. The Greater Beijing Area belongs to the East Asian monsoon region, and its precipitation occurs mainly in summer due to the impact of the summer monsoon from the Pacific Ocean. Therefore, the events were selected from the summers of 2011–2013. According to the CHMPA-Hourly precipitation product, the daily average precipitation amounts for the summers of 2011 to 2013 in the Greater Beijing Area are shown in Fig. 11. To obtain more reasonable validation results, the 20 selected events framed by the boxes marked with numbers (1–20) were simulated by WRF models with both default and optimal parameter values. Finally, Fig. 12 shows a comparison of the TS values of precipitation simulations using optimal and default parameters. Similarly to previous results, the simulations with the optimal parameters enhanced the accuracy of precipitation forecasting. The percentage improvements for light rain, moderate rain, heavy rain, and storm were 1.61, 7.15, 2.10, and 9.44%, respectively. About 70% of the forecasts for the four types of precipitation were improved using the simulations with optimal parameters. For the rest

Fig. 9 Comparison of TS values of four types of precipitation simulations using optimal and default parameters for the validation events from 2008 to 2010

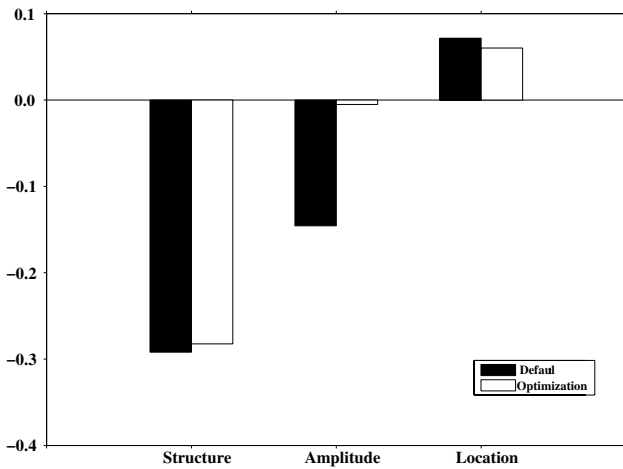
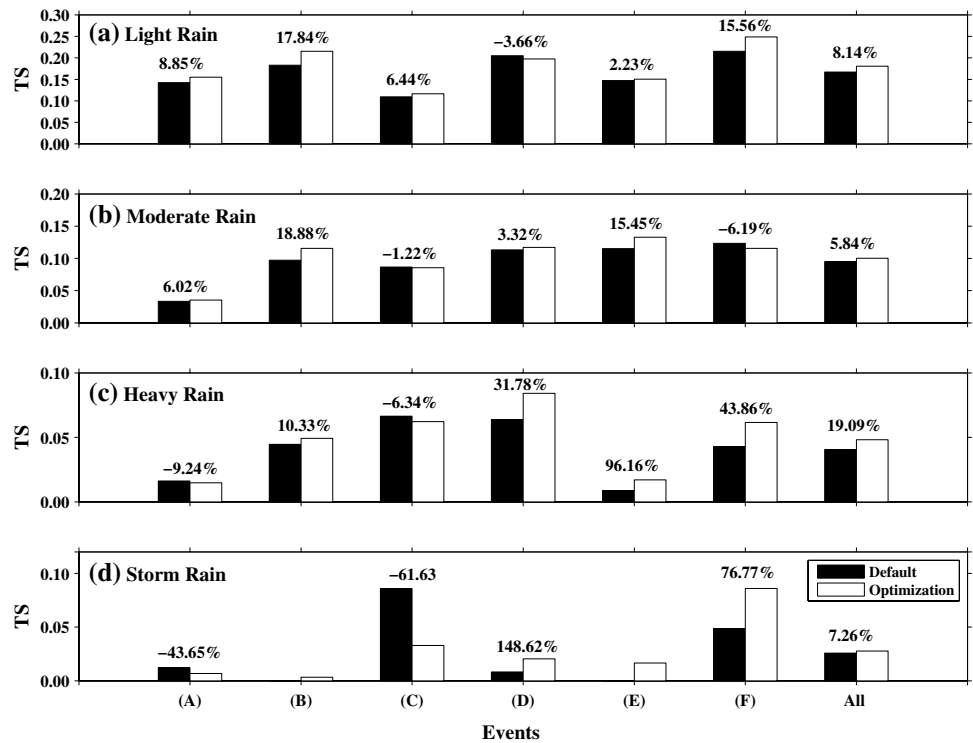


Fig. 10 Same as Fig. 8 except for the validation events from 2008 to 2010

of the forecasts with negative improvement rates, most of them had less than 10% losses in accuracy, and the losses greater than 10% occurred mainly in the forecasts with lower TS values, meaning that the effect of these negative improvement rates on total TS variability was weak. Therefore, it has been demonstrated that the optimal parameters were superior to the default parameters for precipitation simulations from 2011 to 2013, even when more precipitation events were selected to conduct the validation experiments. Overall, we think that the optimal parameters were

proved to be robust for precipitation simulations from the different years.

4.3 Impact of the optimal parameters on precipitation event simulations with other boundary conditions

To assess the transferability of the optimal parameters across different boundary conditions, two reanalysis data, NCEP-FNL (Final) data with a 1.0° grid in latitude and longitude and ECMWF Re-Analysis (ERA)-interim data with a 0.5° grid in latitude and longitude, were used to drive the simulations of summer precipitation events from 2011 to 2013 over Greater Beijing Area besides the CFSR data driving the previous WRF simulations. For the two simulation experiments, the WRF model configurations, the simulation area, and the simulated precipitation events were identical with those of the validation experiments from 2011 to 2013 (see Sect. 4.2.2), except for the boundary conditions. One simulation experiment adopted the NCEP-FNL data as the boundary conditions, and the other experiment used the ERA-interim data as their boundary conditions. We mainly compared the difference of precipitation simulation results from the WRF model with default and optimized parameter values under a new boundary condition.

With the NCEP-FNL data as lateral boundary conditions, Fig. 13 compares the TS values of the two simulations using optimal and default parameter values on precipitation events of 2011–2013. Overall, the TS values of the optimized

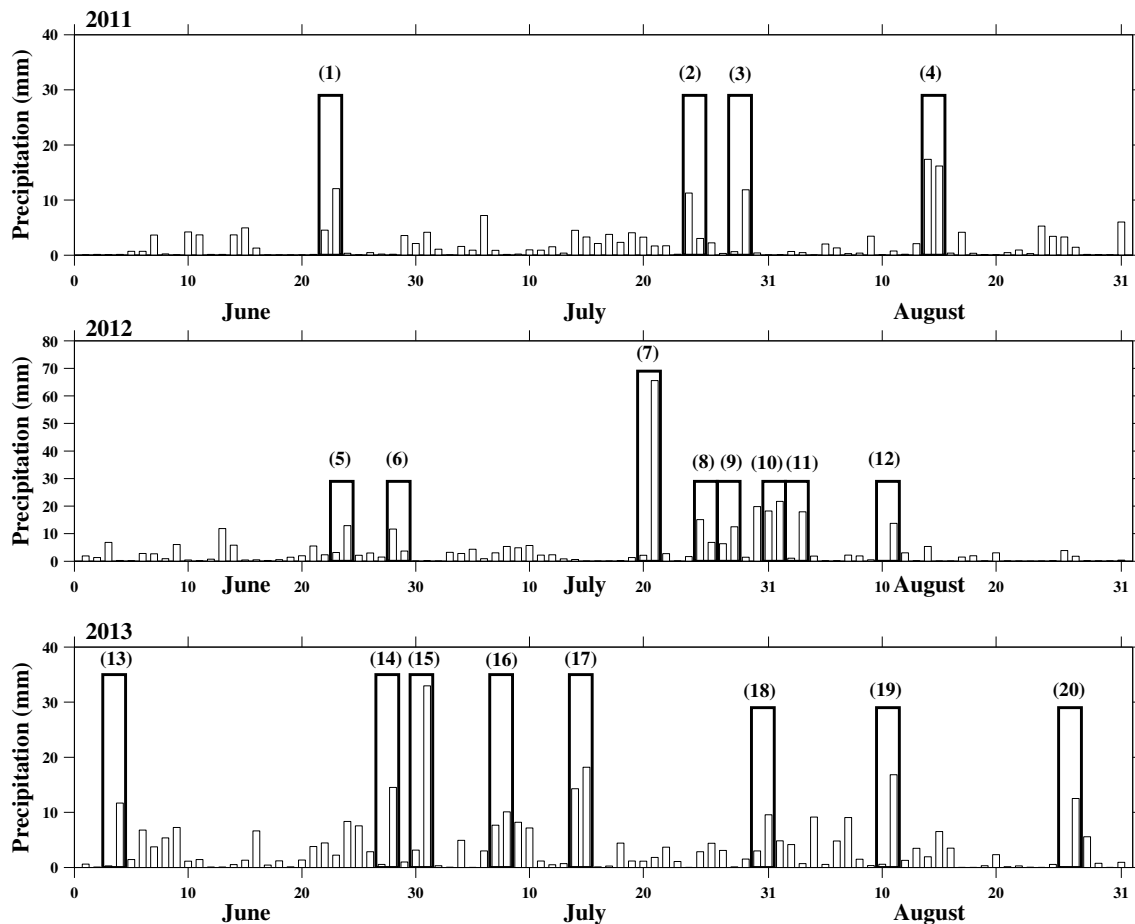


Fig. 11 The 20 precipitation events during the summer in the Greater Beijing Area from 2011 to 2013

simulations were significantly improved over the default simulations. The percentage improvements for light rain, moderate rain, and heavy rain were 4.83, 6.08, and 6.63%, respectively. Although the improvement for the storm simulations was negative using the optimal parameters, the authors concluded that a decrease of -1.69% will not have significantly detrimental effects on storm simulations with the default parameter values. Moreover, only one-sixth of the 80 classification precipitation forecasts [i.e., light rain in events (5) and (6); moderate rain in events (7), (11), and (14); heavy rain in events (4), (5), and (12); and storm in events (1), (4), (5), (6), (11), (14), and (20)] showed significantly weakened trends, which does not change the conclusion that the WRF model with the optimal parameters calibrated by ASMO can obtain still better precipitation forecasts for the Greater Beijing Area even if the boundary conditions were replaced from CFSR to NCEP-FNL.

When the WRF simulations over summer precipitation events of 2011–2013 in Greater Beijing Area were drove by the ERA-interim data instead of CFSR data, the difference of precipitation skill scores for WRF simulations using

optimal and default parameter values was also compared. The corresponding results were shown in Fig. 14. Overall, the percentage improvements for light rain, moderate rain, heavy rain, and storm were 3.18, -0.86 , 11.02, and 12.77%, respectively. The TS results of WRF simulations with the optimal parameters are better than that with the default parameters, especially for the events of heavy rain and storm. There was a little negative improvement for moderate rain, but -0.86% losses would not produce the large destroy to the moderate rain simulations of WRF model with the default parameter values. For all single precipitation events, about one-eighth of the 80 classification precipitation forecasts [i.e., light rain in events (17) and (20); moderate rain in events (7) and (20); heavy rain in events (15) and (19); and storm in events (12), (16), (17), (19), and (20)] showed significantly weakened trends. Another one-tenth of the 80 classification precipitation forecasts showed less than 5% losses. Therefore, we think that the optimal parameters obtained by calibration experiments are superior to the default parameters for WRF summer precipitation simulations even for ERA-interim data as a new boundary.

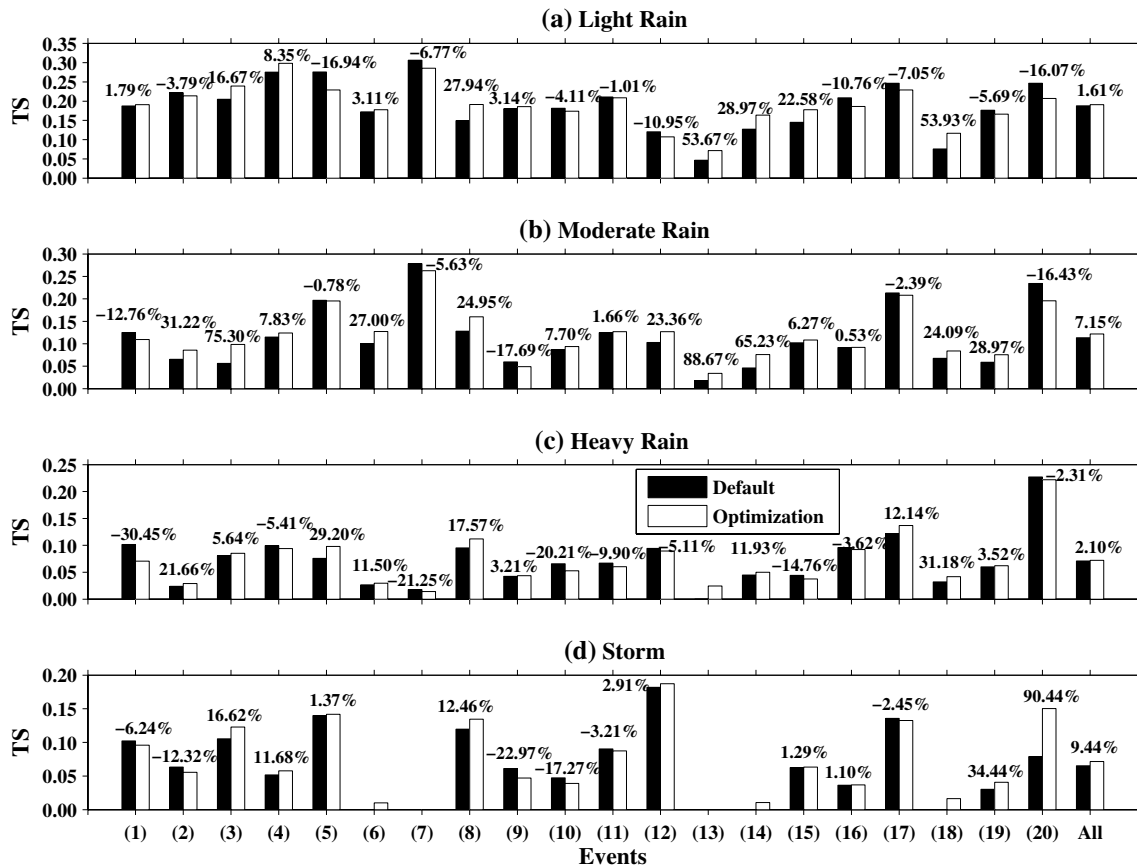


Fig. 12 Comparison of TS values for the four types of precipitation simulations using optimal and default parameters for precipitation events in the Greater Beijing Area from 2011 to 2013

Generally speaking, from the previous comparison experiments using three reanalysis data (CFRS, NCEP-FNL, and ERA-interim) as the boundary conditions respectively, it can be concluded that the optimal parameters are independent of boundary conditions for summer precipitation simulations of the Greater Beijing Area. Moreover, the conclusions obtained by the simulations of 20 precipitation events are convincing.

4.4 Impact of the optimal parameters on precipitation event simulations with the different spatial resolutions

To examine the applicability of the optimal parameters on precipitation event simulations at different spatial resolutions, the same experimental design was used as for the parameter calibration period for the Greater Beijing Area, except for the spatial resolution of the simulations. It refers to two WRF simulations with different spatial resolutions, including a two-layer nested WRF simulation with 3-km spatial resolution in inner layer and 9-km spatial resolution in outer layer (i.e., the previous calibration simulation

called as Run1) and a one-layer WRF simulation with a spatial resolution of 9 km (i.e., called as Run 2). The two WRF simulations had common default parameter values. They were used to simulate summer precipitation events in the Greater Beijing Area. Here, the common simulated precipitation events included events (a–i) from the calibration period and events (A–F) from the validation period in the summers from 2008 to 2010 (see Fig. 2). The common initial and boundary conditions were derived from CFRS data. We first validated the applicability of optimal parameters from Run 1 with high-spatial resolution for improving precipitation forecasts of Run 2 with low-spatial resolution. The optimal parameters of Run 1 adopted that of the previous calibration experiments. Then, the optimization for Run 2 was conducted to obtain the optimal parameters of low-resolution simulation by ASMO. After that, the optimal parameters of Run 2 were put into Run 1 to validate whether they are still superior to corresponding default parameters for improving WRF high-resolution precipitation simulations. Finally, the optimal parameter values of Run 1 and Run 2 were compared to check their consistency.

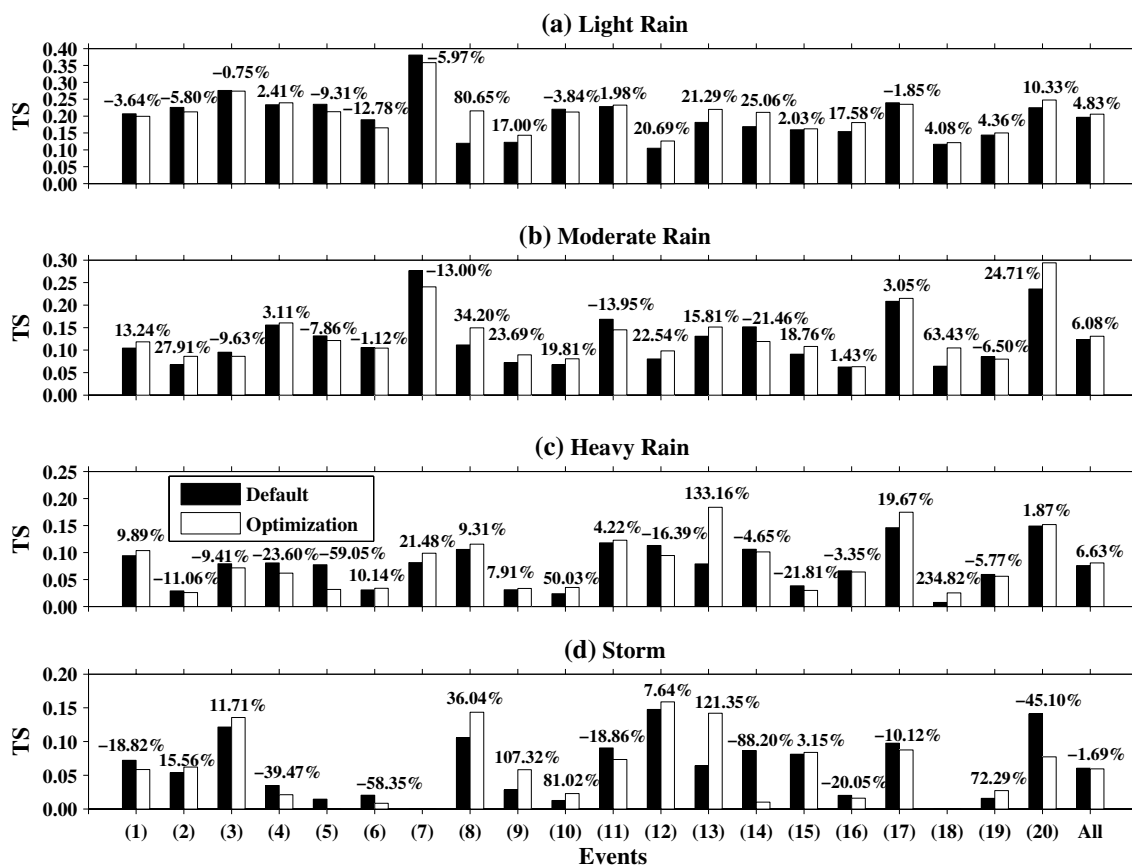


Fig. 13 Same as Fig. 12 except for NCEP-FNL reanalysis data as the boundary conditions

4.4.1 A comparison of Run 2 using default and optimal parameters of Run 1

The optimal parameters of Run 1 obtained by previous calibration experiments were put in a one-layer WRF simulation with 9-km spatial resolution (i.e., Run 2) to compare their simulation results with the corresponding default simulations. Figure 15 shows the comparison results of Run 2 with default and optimal parameters of Run 1. Clearly, Run 2 with optimal parameters of Run 1 has better precipitation simulation capability than that with default parameters. Overall, compared to the Run 2 with default parameters, the Run 2 with optimal parameters of Run 1 improved the TS values for light rain, moderate rain, heavy rain, and storm by 10.19, 4.21, 4.52, and 1.12%, respectively. Figure 15 also shows that one-third of the 60 classification precipitation forecasts had negative increments, and half of these had less than 5% losses in accuracy, which proves that the optimal parameters of Run 1 are superior overall to the default parameters for improving single precipitation forecasts in Run 2. This result demonstrates the superiority of the optimal parameters from the high spatial resolution

simulations for improving precipitation simulations with low spatial resolution in the Greater Beijing Area.

4.4.2 A comparison of Run 1 using default and optimal parameters of Run 2

Firstly, the optimal parameters of Run 2 for the summer precipitation events of 2008–2010 needed to be obtained by re-conducting ASMO method. Based on the 100 initial samples, the optimization convergence criteria were met after 55 adaptive sampling using ASMO. The total weighted objective function values for the four precipitation types decreased from -1 with the default simulation to -1.088 with the optimal simulation. After that the optimal parameters of Run 2 were obtained, it was applied to Run 1 for validating whether the optimal parameters are still superior to corresponding default parameters for improving WRF high-resolution precipitation simulations. The TS values of Run 1 with default parameters and optimal parameters of Run 2 were shown in Fig. 16. Overall, the percentage improvements for the simulations of light rain, moderate rain, and heavy rain are 7.62, 11.71, and 14.07%, respectively. Note also that the simulated average TS

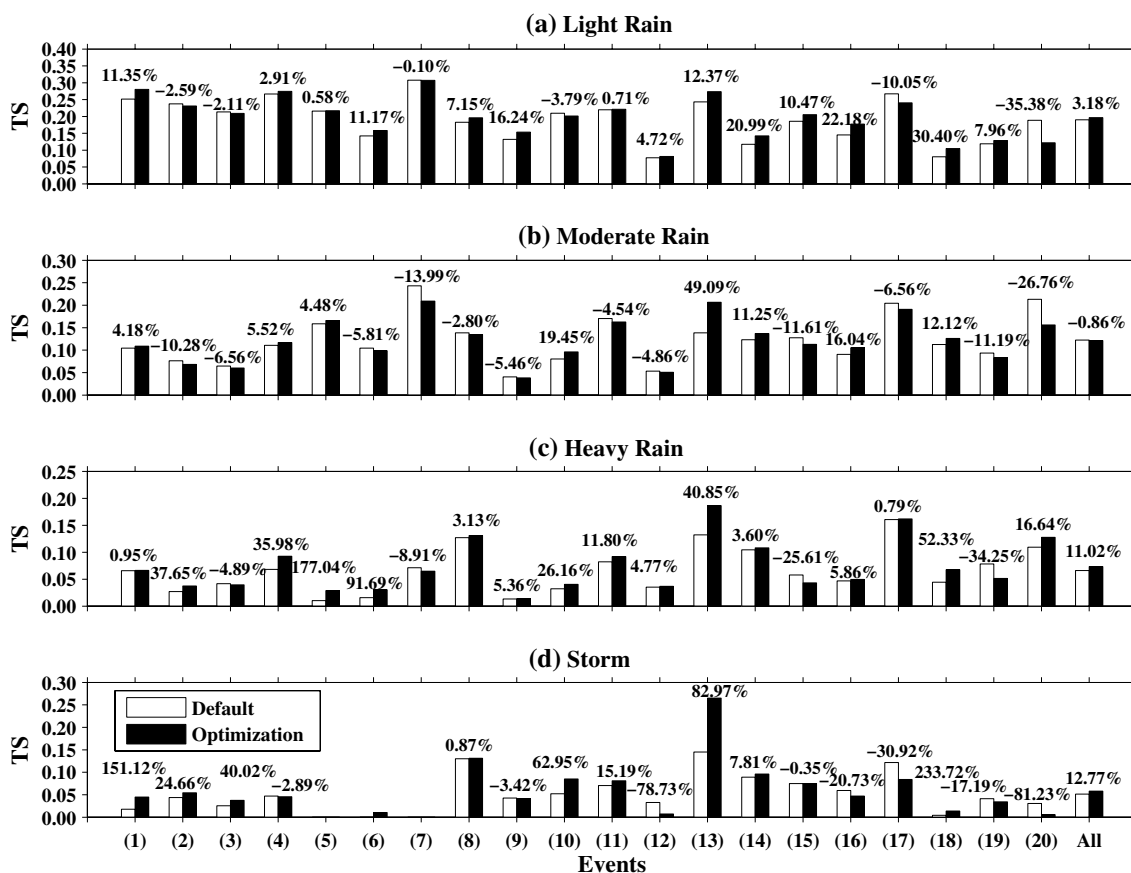


Fig. 14 Same as Fig. 12 except for ERA-interim reanalysis data as the boundary conditions

value of storm has a 2.88% loss for optimization simulation, but the decrease can be also accepted compared with corresponding default simulation. As a whole, the optimal parameters of Run 2 were superior to the corresponding default parameters in Run 1 for summer precipitation event simulations over Greater Beijing Area.

4.4.3 Comparison of two sets of optimal parameters

Three sets of parameters (i.e., default parameters, optimal parameters for Run 1, and optimal parameters for Run 2) were put into Run 1 to conduct their simulated results for precipitation events of 2008–2010 in Greater Beijing Area, respectively. The comparison results of the average TS values for four types of precipitation simulations using three sets of parameters were shown in Fig. 17. Both of the optimization results are significantly superior to the default simulation results for light rain, moderate rain, and heavy rain. However, note that the storm simulation with optimal parameters from Run 1 are slightly better than that with the default parameters, and the storm simulation with optimal parameters from Run 2 are slightly weaker than default simulation. As the whole, both of optimal parameters bring

the better precipitation simulation results compared with the simulation results using default parameters. We also found that the simulated TS values using optimal parameters of Run 2 were higher than those using optimal parameters of Run 1, especially for moderate rain and heavy rain. That is mainly due to the fact that the validation experiments were conducted by Run 1. So, the optimization effect using optimal parameters of Run 1 is more obvious.

Three sets of parameters were also normalized to examine the difference of the two sets of optimal parameters and the difference between optimal parameters and defaults parameters, where the maximum value is 1 and the minimum value is 0. The normalized values for three sets of parameters were shown in Fig. 18. Except for three parameters (i.e., *nOr*, *dimax*, and *sm*), there is an obvious difference of the optimal parameter values for Run 1 and Run2. The inconsistency of two sets of optimal parameter values may be the reason that the truly global optimal solution are not found due to limited optimization researches used. However, the whole variation trend of two sets of optimal parameters is basically consistent compared to the default parameter set. Although the opposite trends exist in parameter of *bsw*, it is not crucial for altering the simulation results because the

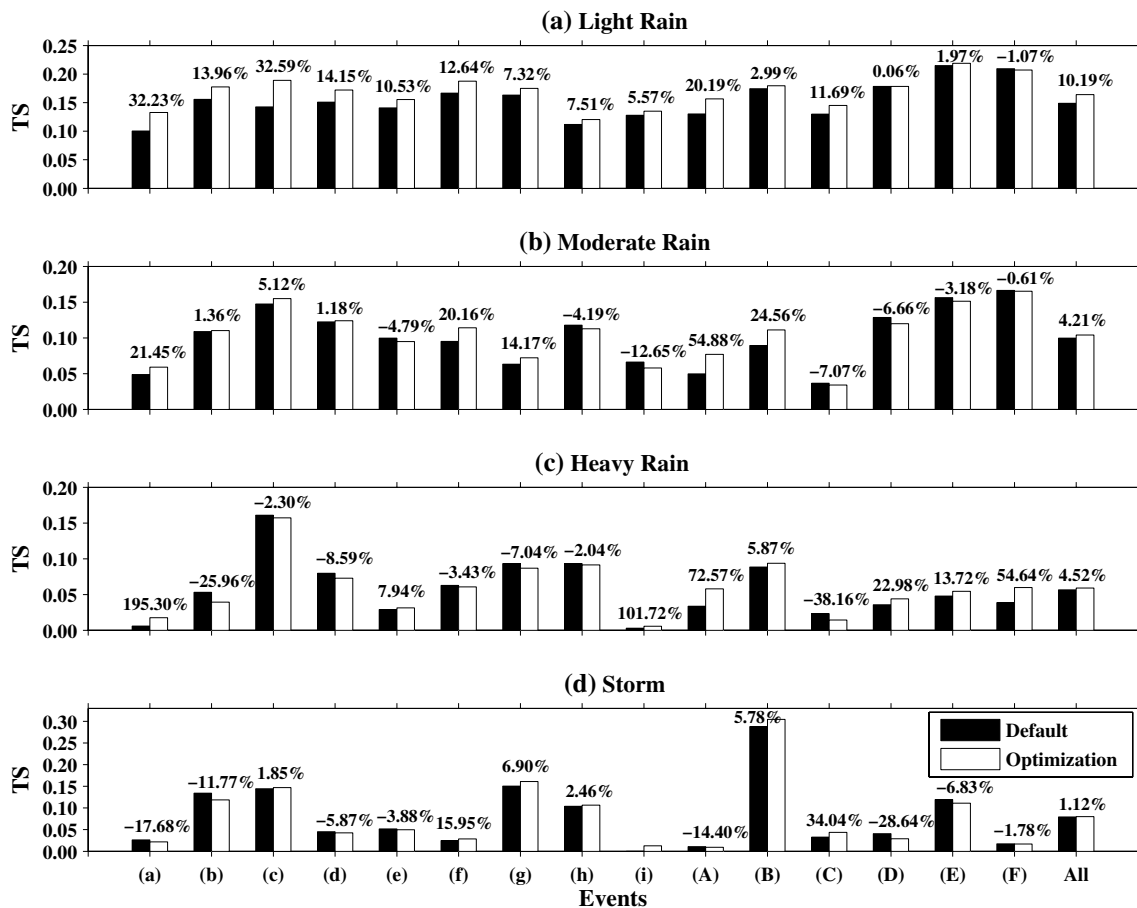


Fig. 15 Comparison of TS values of one-layer WRF simulation with 9-km resolution (i.e., Run 2) for the four types of precipitation using default and optimal parameters of calibrated WRF simulation with

two-layer nested and 3-km spatial resolution in inner layer (i.e., Run 1) for 15 precipitation events in the Greater Beijing Area from 2008 to 2010

sensitivity of *bsw* is weakest in all nine optimized parameters (Di et al. 2016). The consistent trend proved the reasonability of two sets of optimal parameters to some extent.

Overall, compared with the default parameter set, both of two sets of optimal parameters had demonstrated the superiorities for the two simulations with 3 and 9-km spatial resolutions (i.e., Runs 1 and 2). So, it can be concluded that the optimal parameters are independent of spatial resolution for summer precipitation simulations of the Greater Beijing Area.

4.5 Impact of the optimal parameters on simulations of other variables

In this study, the optimal parameters were obtained by constraining the WRF precipitation simulations to the corresponding observations using the ASMO method. The question then arises of how other simulated variables may vary when the optimal precipitation simulation parameters

are used. Using the experimental designs of the calibration period, both 2-m air temperature and 10-m wind speed were simulated by the WRF model with both optimal and default precipitation simulation parameters. Then the differences between the simulation results for 2-m air temperature (10-m wind speed) with optimal and default parameters were compared.

Figure 19 shows the difference between the simulated biases for 2-m air temperature (10-m wind speed) with optimal and default parameters. The simulated results for both temperature and wind speed with the optimal parameters were significantly improved over those with the default parameters, especially for the regions with the highest precipitation amounts (see Fig. 6a), where the precipitation simulations with the optimal parameters showed significant improvement. This shows that the optimal parameters obtained by optimizing the precipitation simulation results are also superior to the default parameters for simulating 2-m air temperature and 10-m wind speed.

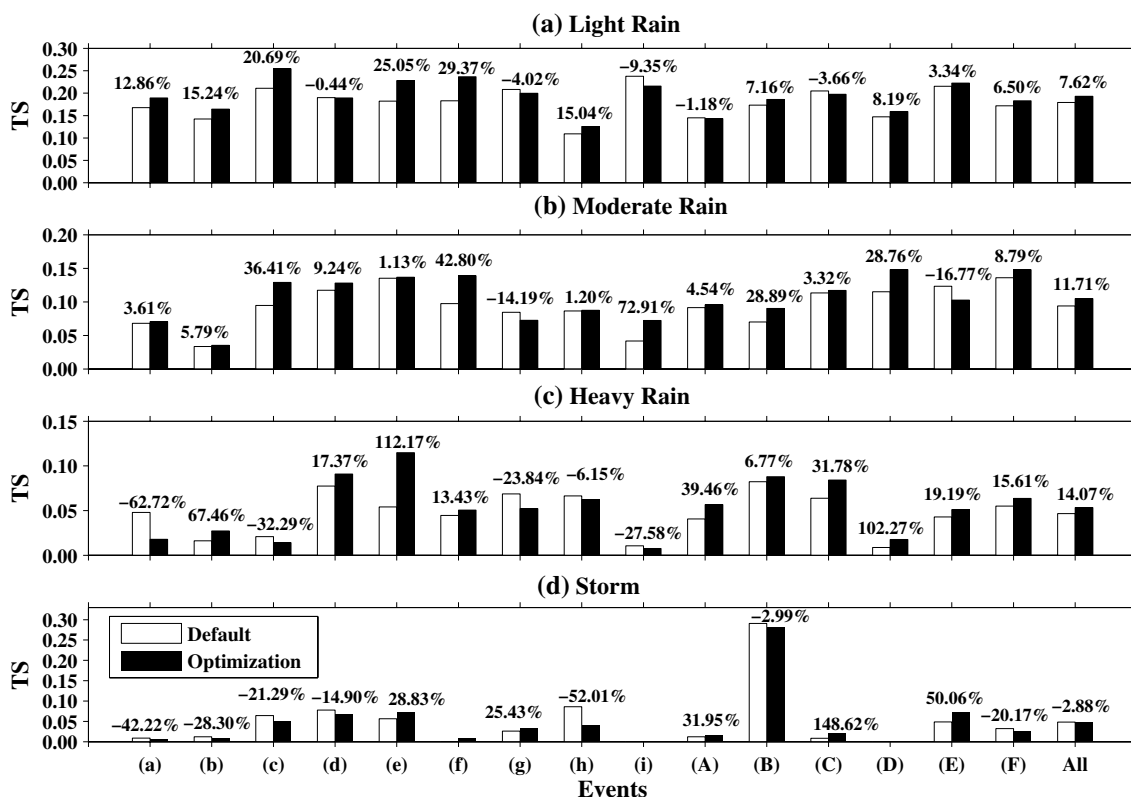


Fig. 16 Comparison of TS values of Run 1 for the four types of precipitation using default and optimal parameters of Run 2 for 15 precipitation events in the Greater Beijing Area from 2008 to 2010

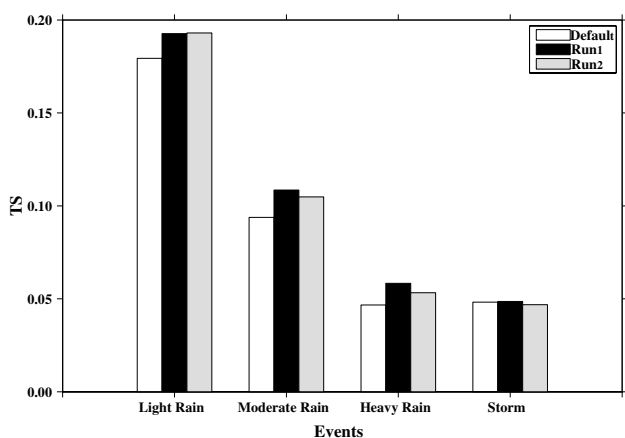


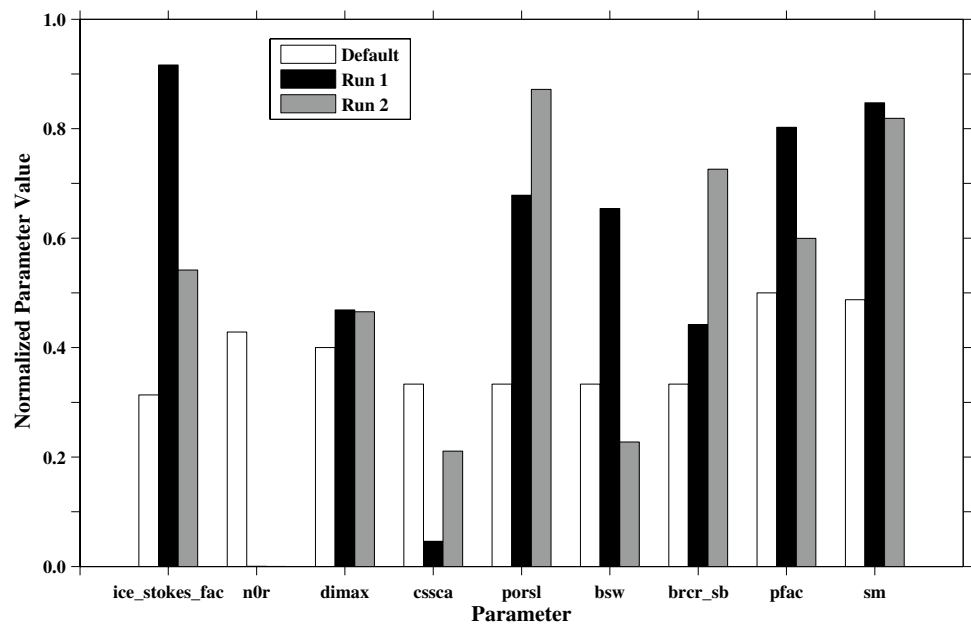
Fig. 17 Comparison of average TS values of Run 1 for four types of precipitation using the three sets of parameters (i.e., default parameters, optimal parameters of Run 1, and optimal parameters of Run 2)

4.6 Physical interpretation of the parameter optimization results

It is shown in Fig. 18 that the variation trends for all the parameters between default and optimal values are inconsistent. This occurred because precipitation is a

comprehensive result of highly nonlinear interactions among various physical processes such as convergence or divergence of water vapor, uplifting and down-drafting of moist air, turbulent exchanges of water and heat fluxes in the surface layer. The *ice_stokes_fac* (Scaling factor applied to ice falling velocity) and *dimax* (Limiting maximum value for the cloud-ice diameter) parameters have jointly positive effects on fallout of ice crystals, and an increase in this factor strengthens conversion from cloud ice to rain water, resulting in a precipitation increase. A decrease in *nDr* (Intercept parameter of rain) means a decrease in rain concentration, which easily produces oversaturation of cloud water and enhances rain sedimentation through the increased mean size of rain aggregates. A lower value for the *cssca* parameter (Scattering tuning parameter) means less scattering of solar radiation in the atmospheric layer, which enhances the amount of shortwave radiation reaching the surface and then the evaporation from the ground, ultimately leading to an increase in precipitation. A higher value for the *porsl* parameter (Multiplier for saturated soil water content) means greater soil porosity between the groundwater surface and the ground surface. This leads to stronger conveyance of soil water upward and thus enhanced

Fig. 18 Comparison of normalized values for three sets of parameters



surface evapotranspiration, which is helpful for the development of precipitation. Higher values for the *bsw* parameter (Multiplier for the Clapp and Hornberger “b” parameter) can also enhance surface evapotranspiration by increasing the conductivity of water and heat in soil layers. Its effect is similar to that of *porsl*. The *brcr_sb* (Critical Richardson number for the boundary layer of land) and *pfac* (Profile shape exponent used to calculate the momentum diffusivity coefficient) parameters have a positive effect on the heat and momentum diffusivity coefficients, respectively. When the values of these two parameters increase, the eddy turbulence diffusivity intensity is enhanced, uplifting heat and water vapor from the ground surface and strengthening convection formation. The *sm* parameter (Counter-gradient proportional coefficient of non-local momentum flux) is used to compute the counter-gradient term, which is a supplement to the local gradient by incorporating the contribution of large-scale eddies to the total flux. Therefore, a higher *sm* value enhances the supply of local eddies in the mixed layer, strengthening the upward transfer of heat and water vapor from the ground surface.

5 Summary and discussion

This study first optimized the nine sensitive parameters of the WRF model using the ASMO method to improve summer precipitation simulations in the Greater Beijing Area. Then, the applicability of the optimal parameters to WRF simulations of the region across precipitation events, boundary conditions, spatial scales, and physical

processes was examined. The selected nine parameters had been obtained from previous parametric sensitivity analysis results for the WRF summer precipitation simulations in the Greater Beijing Area. Multiple precipitation events from 2008 to 2013 were simulated to constrain and verify the optimal WRF model parameters. Each event spanned 2 days. The TS metric was used to evaluate the precipitation simulation results during optimization and validation.

The optimization results showed that precipitation forecasting can be significantly improved by optimizing the WRF model parameters using ASMO, especially for areas of high precipitation. Moreover, 127 adaptive samples achieved convergence of the total normalized TS of the precipitation event simulations during the calibration period, which demonstrates that the ASMO method is very highly efficient. The WRF model with the optimal parameters calibrated by optimizing precipitation simulations for 2008–2010 was also used to simulate precipitation events for 2011–2013. The results show that the optimized parameters can significantly improve the precipitation results over the simulated results of the WRF model with default parameters, which has been demonstrated by various metrics (TS and SAL). So, the optimal parameters were suitable to WRF precipitation simulations for other years. With the boundary conditions replaced, the optimal parameters can still improve precipitation simulations. Three reanalysis data including CFSR data, NCEP-FNL data, and ERA-interim data were used to drive the WRF precipitation simulations from 2011 to 2013, respectively. For each reanalysis data as boundary conditions, the optimal parameters had demonstrated their superiority for WRF precipitation simulations compared to default parameters, which shows

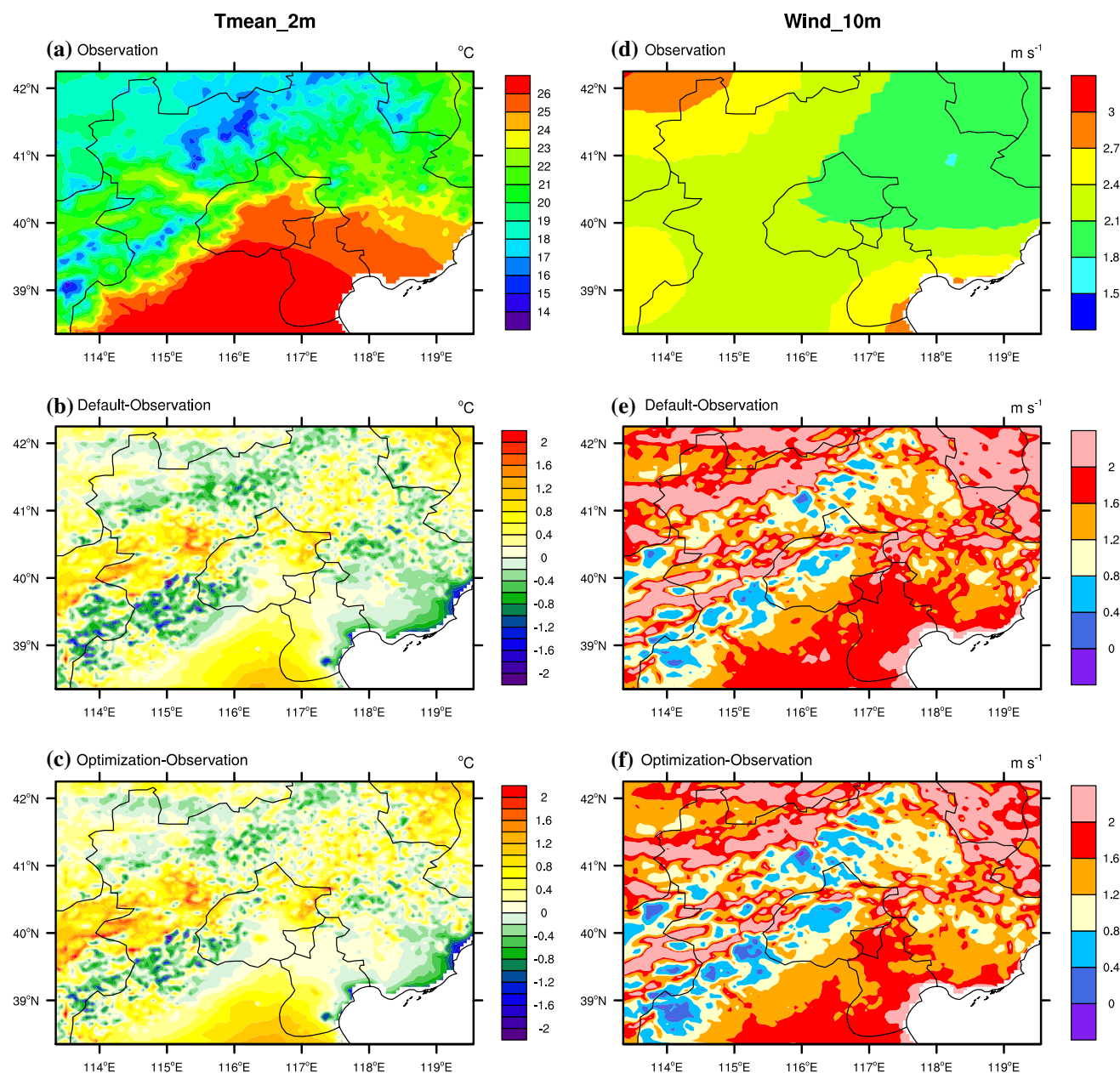


Fig. 19 Spatial comparisons of simulated temperature (*left*) and wind speed (*right*) using optimal and default parameters for the calibration events from 2008 to 2010

that the optimal parameters are independent of boundary condition. With the spatial resolution varied, the optimal parameters can still improve precipitation simulations. Two sets of optimal parameters were obtained from the WRF simulation with 3 and 9-km spatial resolutions, respectively. Not only had the optimal parameters from WRF simulation with 3-km resolution proved their superiority to default parameters for WRF simulation results with 9-km resolution in the Greater Beijing Area, but also the optimal parameters from WRF simulation with 9-km resolution had proved their superiority to default parameters for WRF

simulation results with 3-km resolution over the region. The comparison showed that the optimal parameters are independent of spatial resolution for WRF simulations. Although the optimal parameters were obtained by constraining precipitation simulations alone, the simulations of other output variables such as temperature and wind speed were also improved using the optimal parameters, especially for high-precipitation regions. These assessments of the optimal parameters not only fully prove the reasonableness of the optimal WRF model parameters for improving summer precipitation simulations over the Greater Beijing

Area, but also the feasibility of the ASMO method for optimizing the parameters of the large and complex WRF model.

However, certain limitations remain on parameter optimization in this study. First, the model setup did not fully conform to operational settings. For instance, to reduce input errors, the initial and boundary values in the operational model were assimilated by merging the observed data once every 6 h. Moreover, more than three layers nested simulations were used to obtain more accurate forecasting for the innermost layer. The two-layer nested simulations used in this study were designed out of consideration for available computing resources. These factors could have caused differences between the optimal parameter values of the calibrated WRF model in this study and those of the operational WRF forecasting system. For this reason, it might be better to recalibrate the WRF model parameters for new operational forecasting systems using the ASMO method. Second, the objective function in the WRF model parameter optimization dealt only with precipitation magnitude. A better objective function for optimizing precipitation should also constrain other variables related to precipitation, such as planetary boundary layer height, total precipitable water, cloud cover, and shallow convective mass fluxes. If more variables were simultaneously constrained in the objective function, this would help to obtain more reasonable optimization results for precipitation. To solve such a function, a multiple-objective optimization method would have to be used to produce the Pareto optimal parameter sets. In addition, the spatial correlation coefficient should also be added to the set of metrics for objective functions in future studies besides the magnitudes (e.g., RMSE, TS). Finally, the parameter optimization described here reflected local characteristics. If the optimal parameters in this study were updated to the WRF model for precipitation simulations over other regions with drier climate regimes, such as desert or colder climate regimes, such as the South Pole, the superiority of the optimal parameters would not be retained. Therefore, parameter screening and optimization of sensitive parameters for WRF model would have to be re-implemented to obtain optimal parameter values over the new region.

Acknowledgements This research was supported by the Inter-governmental Key International S&T Innovation Cooperation Program (No. 2016YFE0102400), the Special Fund for Meteorological Scientific Research in the Public Interest (No. GYHY201506002, CRA-40: 40-year CMA global atmospheric reanalysis), the National Basic Research Program of China (No. 2015CB953703), the National Natural Science Foundation of China (No.41305052), and the Fundamental Research Funds for the Central Universities-Beijing Normal University Research Fund (No. 12500-310421103). We acknowledge CFSR reanalysis dataset (<http://nomads.ncdc.noaa.gov/modeldata/>), NCEP reanalysis dataset (<http://rda.ucar.edu/datasets/ds083.2/>),

ERA-interim reanalysis dataset (<http://apps.ecmwf.int/datasets/>) and validation data of China Hourly Merged Precipitation Analysis precipitation products (CHMPA-Hourly, version 1.0. http://data.cma.cn/data/detail/dataCode/SEVP_CLI_CHN_MERGE_CMP_PRE_HOUR_GRID_0.10.html).

References

- Annan JD, Lunt DJ, Hargreaves JC, Valdes PJ (2005) Parameter estimation in an atmospheric GCM using the ensemble Kalman Filter. *Nonlin Processes Geophys* 12(3):363–371. doi:[10.5194/npg-12-363-2005](https://doi.org/10.5194/npg-12-363-2005)
- Barker HW, Pincus R, Morcrette JJ (2002) The monte carlo independent column approximation: application within large-scale models. *Proceedings of the GCSS/ARM workshop on the representation of cloud systems in large-scale models*
- Bellprat O, Kotlarski S, Lüthi D, Schär C (2012) Exploring perturbed physics ensembles in a regional climate model. *J Clim* 25(13):4582–4599. doi:[10.1175/JCLI-D-11-002751](https://doi.org/10.1175/JCLI-D-11-002751)
- Chen F, Dudhia J (2001) Coupling an advanced land surface–hydrology model with the Penn State–NCAR MM5 modeling system part I: model implementation and sensitivity. *Mon Wea Rev* 129(4):569–585. doi:[10.1175/1520-0493\(2001\)129<0569:CAA LSH>20CO;2](https://doi.org/10.1175/1520-0493(2001)129<0569:CAA LSH>20CO;2)
- Cotton WR, Stephens MA, Neuhoff T, Tripoli GJ (1982) The Colorado state university three-dimensional cloud/mesoscale model 1982—part II: an ice phase parameterization. *J Rech Atmos* 16(4):295–320
- Di ZH, Duan QY, Gong W, Ye AZ, Miao CY (2016) Parametric sensitivity analysis of precipitation and temperature based on multi-uncertainty quantification methods in the Weather Research and Forecasting (WRF) model. *Sci China Earth Sci* 60(5):876–898. doi:[10.1007/s11430-016-9021-6](https://doi.org/10.1007/s11430-016-9021-6)
- Duan Q, Sorooshian S, Gupta VK (1994) Optimal use of the SCE-UA global optimization method for calibrating watershed models. *J Hydrol* 158(3–4):265–284. doi:[10.1016/0022-1694\(94\)90057-4](https://doi.org/10.1016/0022-1694(94)90057-4)
- Duan Q, Di Z, Quan J, Wang C, Gong W, Gan Y, Ye A, Miao C, Miao S, Liang X, Fan S (2016) Automatic model calibration—a new way to improve numerical weather forecasting. *Bull Amer Meteor Soc*. doi:[10.1175/BAMS-D-15-00104.1](https://doi.org/10.1175/BAMS-D-15-00104.1)
- Duane GS, Hacker JP (2008) Automatic parameter estimation in a mesoscale model without ensembles. *Nonlinear Time Ser Anal Geosci* 112:81–95. doi:[10.1007/978-3-540-78938-3_5](https://doi.org/10.1007/978-3-540-78938-3_5)
- Dudhia J (1989) Numerical study of convection observed during the winter monsoon experiment using a mesoscale two-dimensional model. *J Atmos Sci* 46(20):3077–3107. doi:[10.1175/1520-0469\(1989\)046<3077:NSOCOD>20CO;2](https://doi.org/10.1175/1520-0469(1989)046<3077:NSOCOD>20CO;2)
- Dudhia J, Gill D, Manning K, Wang W, Bruyere C (1999) PSU/NCAR mesoscale modeling system tutorial class notes and user's guide: MM5 modeling system version 3. NCAR Boulder CO
- Eglese RW (1990) Simulated annealing: a tool for operational research. *Eur J Oper Res* 46(3):271–281. doi:[10.1016/0377-2217\(90\)90001-R](https://doi.org/10.1016/0377-2217(90)90001-R)
- Evensen G (1997) Advanced data assimilation for strongly nonlinear dynamics. *Mon Weather Rev* 125(6):1342–1354. doi:[10.1175/1520-0493\(1997\)125<1342:ADAFSN>20CO;2&nbbsp](https://doi.org/10.1175/1520-0493(1997)125<1342:ADAFSN>20CO;2&nbbsp)
- Gilliam RC, Pleim JE (2010) Performance assessment of new land surface and planetary boundary layer physics in the WRF-ARW. *J Appl Meteor Climatol* 49(4):760–774. doi:[10.1175/2009JAMC21261](https://doi.org/10.1175/2009JAMC21261)

- Gong W, Duan Q, Li J, Wang C, Di Z, Dai Y, Ye A, Miao C (2015) Multi-objective parameter optimization of common land model using adaptive surrogate modeling. *Hydrol Earth Syst Sci* 19:2409–2425. doi:[10.5194/hess-19-2409-2015](https://doi.org/10.5194/hess-19-2409-2015)
- Gong W, Duan Q, Li J, Wang C, Di Z, Ye A, Miao C, Dai Y (2016) Multiobjective adaptive surrogate modeling-based optimization for parameter estimation of large, complex geophysical models. *Water Resour Res* 52:1984–2008 doi:[10.1002/2015WR018230](https://doi.org/10.1002/2015WR018230)
- Gregory D, Morcrette JJ, Jakob C, Beljaars ACM, Stockdale T (2000) Revision of convection, radiation and cloud schemes in the ECMWF integrated forecasting system. *Q J R Meteor Soc* 126(566):1685–1710. doi:[10.1002/qj49712656607](https://doi.org/10.1002/qj49712656607)
- Hong SY, Lim JOJ (2006) The WRF single-moment 6-class microphysics scheme (WSM6), Asia-Pacific. *J Korean Meteorol Soc* 42(2):129–151
- Hong SY, Noh Y, Dudhia J (2006) A new vertical diffusion package with an explicit treatment of entrainment processes. *Mon Wea Rev* 134(9):2318–2341. doi:[10.1175/MWR31991](https://doi.org/10.1175/MWR31991)
- Hou Z, Rubin Y (2005) On minimum relative entropy concepts and prior compatibility issues in vadose zone inverse and forward modeling. *Water Resour Res* 41(411):2179–2187 doi:[10.1029/2005WR004082](https://doi.org/10.1029/2005WR004082)
- Hou Z, Huang M, Leung LR, Lin G, Ricciuto DM (2012) Sensitivity of surface flux simulations to hydrologic parameters based on an uncertainty quantification framework applied to the community land model. *J Geophys Res*. doi:[10.1029/2012JD017521](https://doi.org/10.1029/2012JD017521)
- Huang XY, Xiao Q, Barker DM, Zhang X, Michalakes J, Huang W, Henderson T, Bray J, Chen Y, Ma Z (2009) Four-dimensional variational data assimilation for WRF: formulation and preliminary results. *Mon Wea Rev* 137(1):99–314. doi:[10.1175/2008MWR25771](https://doi.org/10.1175/2008MWR25771)
- Ihshaish H, Cortés A, Senar MA (2012) Parallel multi-level genetic ensemble for numerical weather prediction enhancement. *Proc Comp Sci* 9(11):276–285. doi:[10.1016/j.procs.201204029](https://doi.org/10.1016/j.procs.201204029)
- Jackson CS, Sen MK, Huerta G, Deng Y, Bowman KP (2008) Error reduction and convergence in climate prediction. *J Clim* 21(24):6698–6709 doi:[10.1175/2008JCLI21121](https://doi.org/10.1175/2008JCLI21121)
- Janjic ZI (1994) The step-mountain eta coordinate model: further development of the convection, viscous sublayer, and turbulent closure schemes. *Mon Wea Rev* 122:927–945. doi:[10.1175/1520-0493\(1994\)122<0927:TSMECM>20CO;2](https://doi.org/10.1175/1520-0493(1994)122<0927:TSMECM>20CO;2)
- Jones DR, Schonlau M, Welch WJ (1998) Efficient global optimization of expensive black-box functions. *J Global Optim* 13(4):455–492. doi:[10.1023/A:1008306431147](https://doi.org/10.1023/A:1008306431147)
- Kain JS (2004) The Kain-Fritsch convective parameterization: an update. *J Appl Meteor Clim* 43(1):170–181. doi:[10.1175/1520-0450\(2004\)043<0170:TKCPAU>20CO;2](https://doi.org/10.1175/1520-0450(2004)043<0170:TKCPAU>20CO;2)
- Kalnay E (2003) Atmospheric modeling, data assimilation, and predictability. Cambridge University Press, UK
- Liu DC, Nocedal J (1989) On the limited memory BFGS method for large scale optimization. *Math Progr* 45(45):503–528. doi:[10.1007/BF01589116](https://doi.org/10.1007/BF01589116)
- Liu Y, Gupta HV, Sorooshian S, Bastidas LA, Shuttleworth WJ (2004) Exploring parameter sensitivities of the land surface using a locally coupled land-atmosphere model. *J Geophys Res* 109(D21):2119–2143 doi:[10.1029/2004JD004730](https://doi.org/10.1029/2004JD004730)
- Liu Y, Gupta HV, Sorooshian S, Bastidas LA, Shuttleworth WJ (2005) Constraining land surface and atmospheric parameters of a locally coupled model using observational data. *J Hydrometeor* 6(2):156–172 doi:[10.1175/JHM4071](https://doi.org/10.1175/JHM4071)
- Liu J, Bray M, Han D (2013) Exploring the effect of data assimilation by WRF-3DVar for numerical rainfall prediction with different types of storm events. *Hydrol Process* 27(25):2537–2541 doi:[10.1002/hyp9488](https://doi.org/10.1002/hyp9488)
- Lorenz EN (1960) Energy and numerical weather prediction. *Tellus* 12(4):364–373 doi:[10.1111/j2153-34901960tb01323x](https://doi.org/10.1111/j2153-34901960tb01323x)
- Michielssen E, Ranjithan S, Mitra R (1993) Optimal multilayer filter design using real coded genetic algorithms. *IEE Proc Part J Optoelectron* 139(6):413–420
- Mlawer EJ, Taubman SJ, Brown PD, Iacono MJ, Clough SA (1997) Radiative transfer for inhomogeneous atmospheres: RRTM, a validated correlated-k model for the longwave. *J Geophys Res* 102(D14):16663–16682 doi:[10.1029/97JD00237](https://doi.org/10.1029/97JD00237)
- Mu M, Duan W, Wang J (2002) Nonlinear optimization problems in atmospheric and oceanic sciences. *East-West J Math* 155:169–178
- Nelder JA, Mead R (1965) A simplex method for function minimization. *Comput J* 7(4):308–313. doi:[10.1093/comjnl/74308](https://doi.org/10.1093/comjnl/74308)
- Ollinaho P, Järvinen H, Bauer P, Laine M, Bechtold P, Susiluoto J, Haario H (2014) Optimization of NWP model closure parameters using total energy norm of forecast error as a target. *Geosci Model Dev* 7(7): 1889–1900. doi:[10.5194/gmd-7-1889-2014](https://doi.org/10.5194/gmd-7-1889-2014)
- Qiu CJ, Chou JF (1988) A new approach to improve the numerical weather prediction. *Sci China Ser B* 31(9):1132–1142. doi:[10.1360/yb1988-31-9-1132](https://doi.org/10.1360/yb1988-31-9-1132)
- Rabier F (2005) Overview of global data assimilation developments in numerical weather-prediction centers. *Q J R Meteorol Soc* 131:3215–3233 doi:[10.1256/qj05129](https://doi.org/10.1256/qj05129)
- Richardson LF (2007) Weather prediction by numerical process. Cambridge University Press, UK
- Santanello JA, Kumar SV, Peterslidard CD, Harrison K, Zhou S (2013) Impact of land model calibration on coupled land-atmosphere prediction. *J Hydrometeor* 14(5):1373–1400. doi:[10.1175/JHM-D-12-01271](https://doi.org/10.1175/JHM-D-12-01271)
- Severijns CA, Hazeleger W (2005) Optimizing parameters in an atmospheric general circulation model. *J Clim* 18(17):3527–3535. doi:[10.1175/JCLI34301](https://doi.org/10.1175/JCLI34301)
- Shen Y, Zhao P, Pan Y, Yu J (2014) A high spatiotemporal gauge-satellite merged precipitation analysis over China. *J Geophys Res* 119(6):3063–3075. doi:[10.1002/2013JD020686](https://doi.org/10.1002/2013JD020686)
- Skamarock W, Klemp J, Dudhia J, Gill D, Barker D, Duda M, Huang X, Wang W, Powers J (2008) A description of the advanced research WRF version 3. NCAR Tech Note Mesoscale and Microscale Meteorology Division National Center for Atmospheric Research Boulder Colorado USA
- Wang X, Barker DM, Snyder C, Hamill TM (2008) A hybrid ETKF-3DVAR data assimilation scheme for the WRF model part II: real observation experiments. *Mon Wea Rev* 136(12):5132–5147. doi:[10.1175/2008MWR24441](https://doi.org/10.1175/2008MWR24441)
- Wang C, Duan Q, Gong W, Ye A, Di Z, Miao C (2014) An evaluation of adaptive surrogate modeling based optimization with two benchmark problems. *Environ Modell Softw* 60(76):167–179. doi:[10.1016/j.envsoft.201405026](https://doi.org/10.1016/j.envsoft.201405026)
- Wang C, Duan Q, Tong C, Di Z, Gong W (2016) A GUI platform for uncertainty quantification of complex dynamical models. *Environ Modell Softw* 76:1–12. doi:[10.1016/j.envsoft.201511004](https://doi.org/10.1016/j.envsoft.201511004)
- Wernli H, Paulat M, Hagen M, Frei C (2008) SAL—A novel quality measure for the verification of quantitative precipitation forecasts. *Mon Wea Rev* 136(11):4470–4487. doi:[10.1175/2008MWR24151](https://doi.org/10.1175/2008MWR24151)
- Woodbury AD, Ullrich TJ (1993) Minimum relative entropy: forward probabilistic modeling. *Water Resour Res* 29(8):2847–2860 doi:[10.1029/93WR00923](https://doi.org/10.1029/93WR00923)
- Yan H, Qian Y, Lin G, Leung LR, Yang B, Fu Q (2014) Parametric sensitivity and calibration for the Kain-Fritsch convective parameterization scheme in the WRF model. *Clim Res* 59(2):135–147. doi:[10.3354/cr01213](https://doi.org/10.3354/cr01213)
- Yang B, Qian Y, Lin G, Leung R, Zhang Y (2012) Some issues in uncertainty quantification and parameter tuning: a case study of convective parameterization scheme in the WRF regional climate model. *Atmos Chem Phys* 12(5):2409–2427. doi:[10.5194/acp-12-2409-2012](https://doi.org/10.5194/acp-12-2409-2012)